OF-55

DISCRIMINATION OF HYDROTHERMALLY ALTERED ROCKS ALONG THE BATTLE MOUNTAIN-EUREKA, NEVADA MINERAL BELT USING LANDSAT IMAGES

by

M. Dennis Krohn
U.S. Geological Survey, Reston, Virginia

Michael J. Abrams
Jet Propulsion Laboratory, Pasadena, California

Lawrence C. Rowan
U.S. Geological Survey, Reston, Virginia

1978

U. S. Geological Survey
OPEN FILE REPORT 78-585

TABLE OF CONTENTS

LIST OF FIGURES

LIST OF TABLES

ABSTRACT

Landsat Multispectral Scanner (MSS) images of the northwestern part of the Battle Mountain-Eureka, Nevada mineral belt were evaluated for distinguishing hydrothermally altered rocks associated with porphyry copper and disseminated gold deposits. Detection of altered rocks from Landsat is based on the distinctive spectral reflectance of limonite present at coatings on weathered surfaces. Some altered rocks are visible as bleached areas in individual MSS bands; however, they cannot be consistently distinguished from unaltered rocks with high albedo nor from bright areas resulting from topographic slope. Black-and-white ratio images were generated to subdue topographic effects, and three ratio images were composited in color to portray spectral radiance differences, forming an image known as a color-ratio composite (CRC). The optimum CRC image for this area has MSS 4/5 as blue, MSS 4/6 as yellow, and MSS 6/7 as magenta, and differs in two respects from most CRC images of arid areas. First, as a result of the increased vegetation cover in the study area, MSS 5/6 was replaced by MSS 4/6 as the yellow layer. Second, 70 mm positive transparencies were replaced by large format images (64 cm), thereby improving the internal registration of the CRC image and the effective spatial resolution.

The pattern of limonitic rocks depicted in the CRC closely agrees with the mapped pattern of the alteration zones at the Copper Canyon and Copper Basin porphyry copper deposits. Certain west-facing

topographic slopes in the altered areas are depicted as unaltered in the CRC, apparently due to atmospheric scattering, and illustrate the need for atmospheric correction. The disseminated gold deposits at Gold Acres and Tenabo are poorly represented in the CRC because of the general absence of limonite on these deposits. The presence of unaltered limonitic sedimentary and volcanic rocks is the largest obstacle to discriminating altered areas within the mineral belt. Reflectance spectra, made in situ and in the laboratory indicate differences between altered and unaltered rocks in the spectra region between 1.1 μm and 2.5 μm. Such differences may be detectable by a remote scanner with a longer wavelength range than current Landsat MSS (0.6 μm-1.1 μm).

INTRODUCTION

Landsat Multispectral Scanner (MSS) images have proven to be effective for mapping exposures of limonitic rocks in areas of low vegetation cover. Color composites of ratio images (CRC) can be used to display the distinctive spectral reflectance of limonite while brightness variations resulting from albedo and topographic slope are subdued. This capability is useful for augmenting conventional mineral exploration and assessment methods because of the common association of limonite with iron-sulfide bearing hydrothermally altered rocks. However, the practical application of this mapping technique is reduced where limonitic unaltered rocks and iron-poor altered rocks are common. Using CRC images, Rowan and others (1974, 1977) differentiated between limonitic hydrothermally altered rocks and most unaltered rocks in south-central Nevada; Raines (1976) identified several zones for geochemical exploration in northern Mexico; Blodgett and others (1975) discriminated among rock types in Saudi Arabia; and Vincent (1977) and Offield (1976) have been able to discern iron-oxide stained rocks associated with sedimentary uranium deposits.

The objective of this paper is to evaluate Landsat MSS color-ratio composite images for mapping hydrothermally altered rocks in the vicinity of Battle Mountain, Nevada (fig. 1). The area includes a large part of the Battle Mountain-Eureka mineral belt, a well-known northwest-trending alignment of base and precious metal deposits (Roberts, 1966; Horton, 1966; Shawe and others, 1976) (fig. 2). The study is part of Landsat Follow-on Experiment No. 23890 proposed to

evaluate CRC images at known mineral deposits in the Great Basin of the western United States. The other three sites studied are: (1) the Virginia Range southeast of Reno, Nevada; (2) the East Tintic Mountains southwest of Salt Lake City, Utah; and (3) the south-central Nevada area centered around Tonopah and Goldfield. Results from the other three areas are reported separately.

The study areas were chosen to evaluate CRC images in areas with different geologic and environmental settings from the initial study in south-central Nevada (Rowan and others, 1974). Five factors were identified that might affect identification of hydrothermally altered rocks in CRC images:

1. A variety of hydrothermal alteration types is present in the Battle Mountain-Eureka mineral belt, including potassic, argillic, and siliceous alteration.

2. Host rocks in the mineral belt are dominantly siliceous, Paleozoic sedimentary rocks that are commonly ferruginous, and as such may interfere with the identification of hydrothermally-derived limonite.

3. Many small altered areas and vein deposits are present along the Battle Mountain-Eureka mineral belt for determining effective resolution limits of the MSS ratio images.

4. Desert shrub vegetation forms a moderately dense ground cover that may affect detection of the rock spectral reflectance.

5. The topography of the Battle Mountain and Shoshone Ranges permits checking sun angle effects on the ratio images.

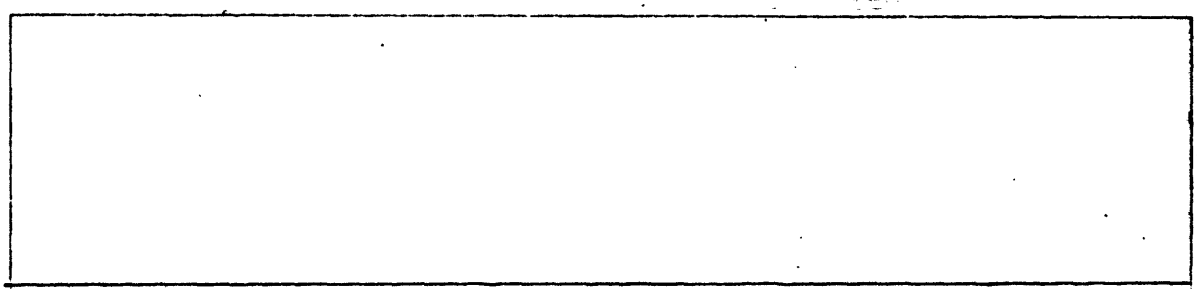

Figure 1 - Index map of the Great Basin physiographic province. Box denotes study area centered about the Battle Mountain-Eureka mineral belt. Numbers locate other study areas in the Great Basin reported elsewhere:

1. Virginia Range, Nevada
2. East Tintic Mountains, Utah
3. South-central Nevada area near Tonopah and Goldfield

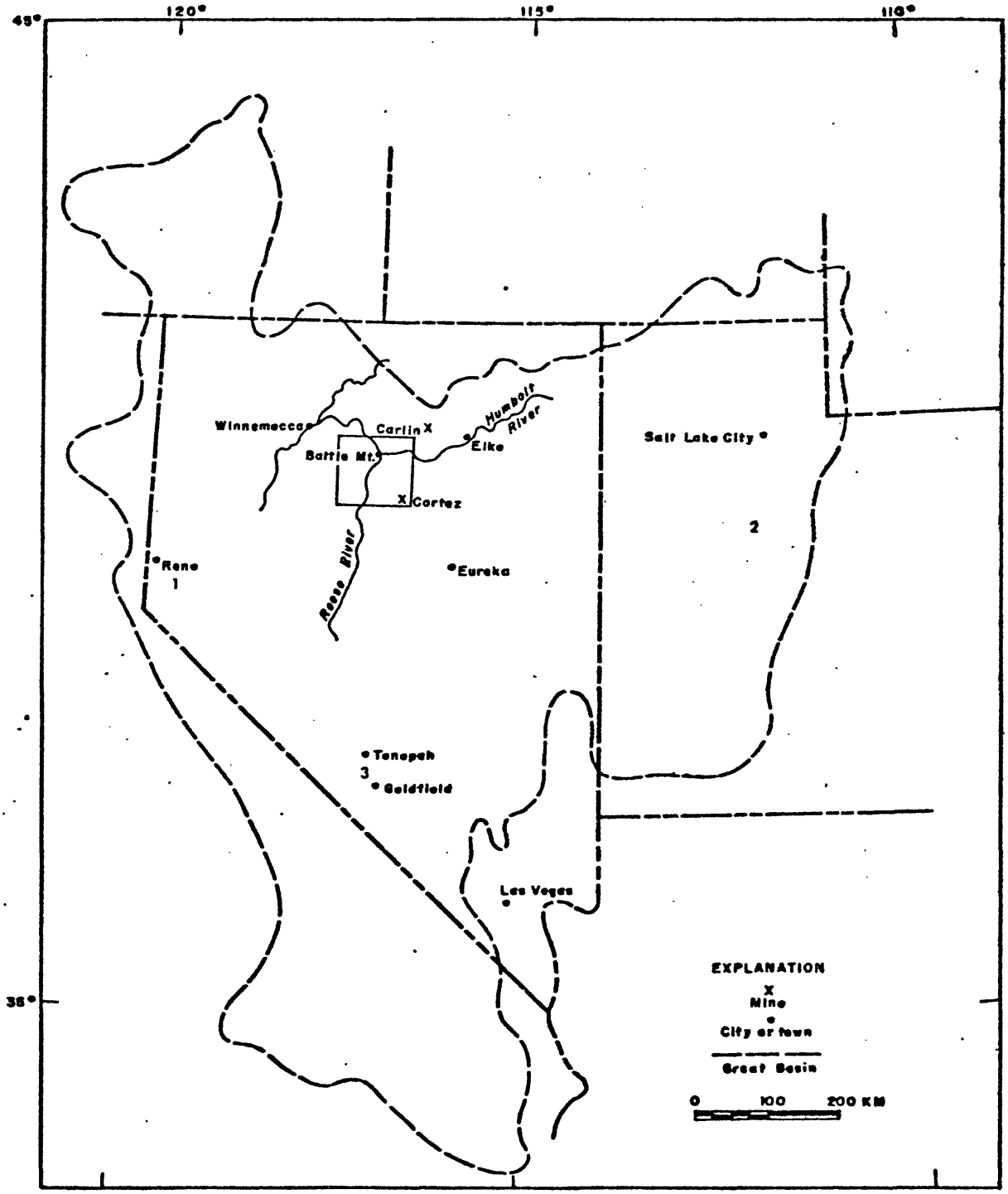
45°
120°
115°
110°
Winnemecca
Carlin
Humboldt River
Elko
Battle Mt.
Cortez
Salt Lake City
2
Reno
1
Reese River
Eureka
Tonopah
3
Goldfield
Las Vegas
38°
EXPLANATION
Mine
City or town
Great Basin
0
100
200 KM

Figure 1.

Figure 2 - Map of major mines and known areas of hydrothermal alteration along the Battle Mountain-Eureka mineral belt. (Modified from Gilluly and Gates, 1965; Roberts and Arnold, 1965; Wrucke, 1974; Theodore and Blake, 1975; Stewart and Carlson, 1976)

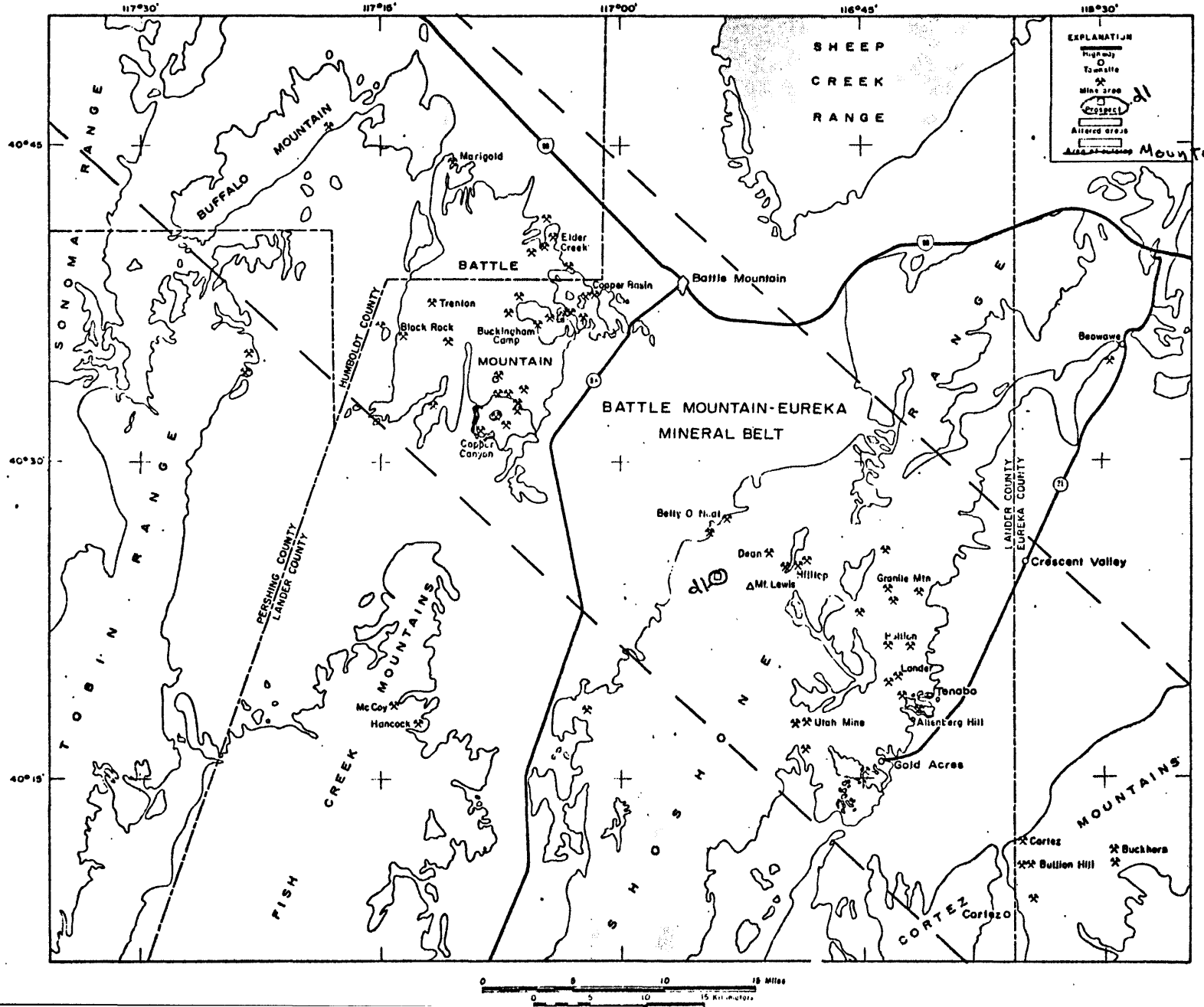
117°30'
117°15'
117°00'
116°45'
118°30'
40°45'
40°30'
40°15'
SHEEP CREEK RANGE
BUFFALO MOUNTAIN
SONOMA RANGE
TOBIN RANGE
SHOSHONE RANGE
FISH CREEK MOUNTAINS
CORTEZ MOUNTAINS
BATTLE MOUNTAIN
HUMBOLDT COUNTY
PERSHING COUNTY
LANDER COUNTY
EUREKA COUNTY
BATTLE MOUNTAIN-EUREKA MINERAL BELT
Marigold
Elder Creek
Copper Basin
Battle Mountain
Trenton
Block Rock
Buckingham Camp
Copper Canyon
Beowawe
Crescent Valley
Dean
Hilltop
Mt. Lewis
Granite Mtn
Londe
Tenabo
Utah Mine
Gold Acres
McCoy
Hancock
Cortez
Buckhorn
Bullion Hill
Cortez
EXPLANATION
Mountain ranges
0 5 10 15 Miles
0 5 10 15 Kilometers

DESCRIPTION OF THE STUDY AREA

Topography

The Battle Mountain study area encloses an 8500 km^2 area of north-central Nevada within the Great Basin (fig. 1). Basin and Range topography dominates the landscape, and mountain ranges rise about 1000 m above the wide intermontane basins (fig 3). Elevation above sea level varies from 1402 m in the basins up to 2905.5 m at the summit of Mt. Lewis in the Shoshone Range (fig. 2). The steepest topography occurs in conjunction with the Basin and Range fuults; slopes up to 412 m/km are present in the western Shoshone Range.

Climate

The climate of north-central Nevada is semi-arid; rainfall averages 15 cm per year with summer precipitation of only 10 cm. Average January temperature is 28°F; average July temperature is 72°F.

Vegetation

Cronquist and others (1972, p. 123) classify vegetation of the Battle Mountain study area in the sagebrush-grass zone. Low desert shrubs, such as big sage, little sage, and rabbitbrush, are interspersed with grasses, and cover from 15 to 40 percent of the ground surface. Cottonwood, chokecherry, and willow are confined to the ephemeral stream canyons, and are visible in Landsat images as lines of vegetation. Associated species and botanical names are presented in Table 1.

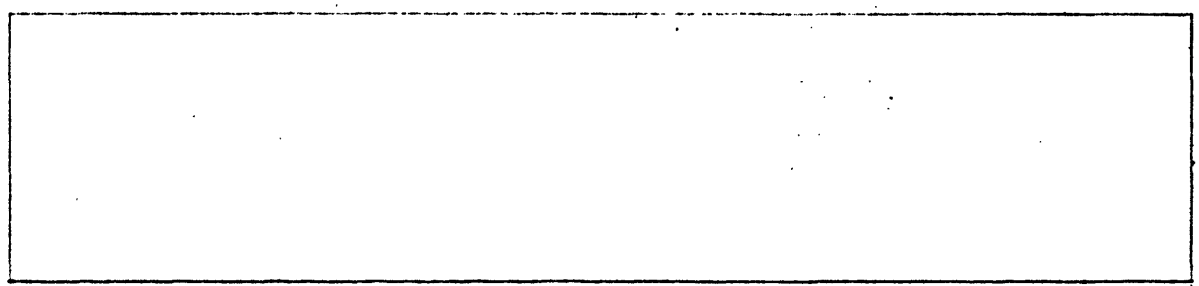

Figure 3 - Landsat color-infrared composite of north-central Nevada including the area of the Battle Mountain-Eureka mineral belt. A, Copper Basin mine; B, Copper Canyon mine; C, Gold Acres mine; D, the town of Battle Mountain; and Tc, the area of Cataeno tuff (between arrows).

Table 1
List of the common plants occurring in the Battle Mountain area
(Preston, 1968; Jaeger, 1969; Reil, 1976, pers. comm.)

Acer negundo	Box elder
Artemesia arbuscula	Little sage
Artemesia spinescens	Bud sage
Artemesia tridentata	Big sage
Atriplex confertiflora	Shadscale
Atriplex sp	Saltbrush
Bromus tectorum	Cheat grass
Chrysothamnus nauseasus	Rubber rabbit brush
Chrysothamnus teretifolius	Terete-leaved rabbit brush
Chrysothamnus viscidiflorus	Sticky-leaved rabbit brush
Halogeton glomeratus	
Juniperus scopulorum	Rocky Mountain juniper
Pinus monophylla	Single leaf pinyon
Populus fremontii	Fremont cottonwood
Populus tremuloides	Quaking aspen
Prunus virginiana	Western choke cherry
Salix sp	Willow
Sarcobatus vermiculatus	Greasewood

The Battle Mountain study area is intermediate in rainfall and vegetation density in comparison to the other three study areas in the Great Basin. The climate at Goldfield is more arid than Battle Mountain, and desert shrubs of the Shadscale zone cover about 10 per cent of the ground (Cronquist and others, 1972, p. 115). Vegetation in the East Tintic Mountains and the Virginia Range are classified in both the sagebrush zone and the juniper-pinyon zone (Cronquist and others, 1972). In general, shrub vegetation appears to be greater ground cover in these two areas than in the Battle Mountain study area; however, the most prominent difference is the large number of pinyon and juniper trees present at Tintic and the Virginia Range.

Vegetation differences can change the spectral representation of rocks in the Landsat images. Juniper and pinyon trees seem to have a greater masking effect than shrub vegetation because they are more reflective in the near-infrared (Milton, unpubl. data). Vegetation in the East Tintic and Virginia Range is sufficiently dense to obscure some areas of hydrothermally-altered rocks. In contrast, the sparse vegetation at Goldfield seems to have little effect on the CRC image. At Battle Mountain, the effect of vegetation on the CRC images falls somewhere in between these two areas.

GEOLOGIC SETTING

Sedimentary Rocks

Siliceous sedimentary rocks are the predominent rock type in the Battle Mountain study area. The Battle Mountain area, therefore, affords an opportunity to study the effect of hydrothermal alteration on dominantly siliceous sedimentary host rocks. Differences in the sedimentary host rocks, such as composition, grain size, and overall fabric can affect the mineral content and type of surface coating present on the hydrothermally altered rocks.

A lithologic map of sedimentary rocks for Battle Mountain (fig. 4) was constructed from published stratigraphic maps (Roberts, 1964) for comparison with the CRC image. Most of the sedimentary rocks in the area are Paleozoic in age; however, the stratigraphy of north-central Nevada is currently undergoing major revision (Stewart and others, 1977; Jones and others, in press). Previously recognized formations and their ages are subject to change. No stratigraphic column is presented here, but the published stratigraphic formation names are used so that the literature can be cited.

Chert. Chert (unit C, fig. 4) covers the largest part of the Battle Mountain area, and includes the Scott Canyon formation, the chert member of the Valmy formation, the Pumpernickel formation, and the Trenton Canyon member of the Havallah formation (Roberts, 1964). The chert is commonly gray-green to black, thin to medium-bedded, and, as shown in figure 4, includes greenstone, dark shale,

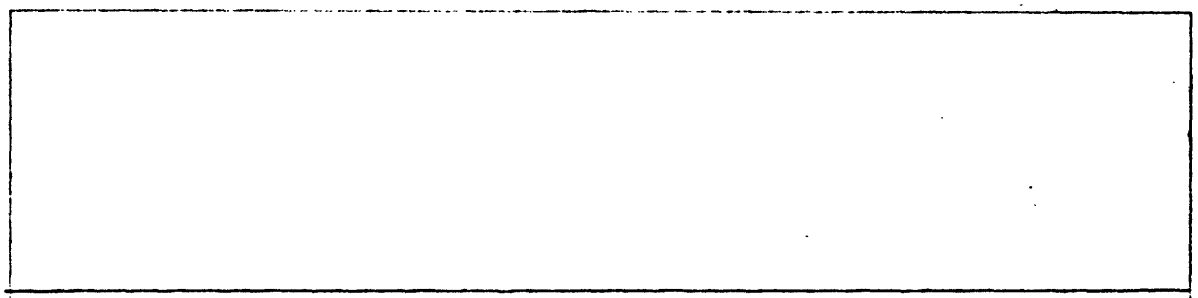

Figure 4 - Map of summarized lithologic units for Antler Peak 15' quadrangle (modified from Roberts, 1964). Lithologic units (particularly chert and quartzite) are summarized from stratigraphic maps, and may encompass other lithologies.

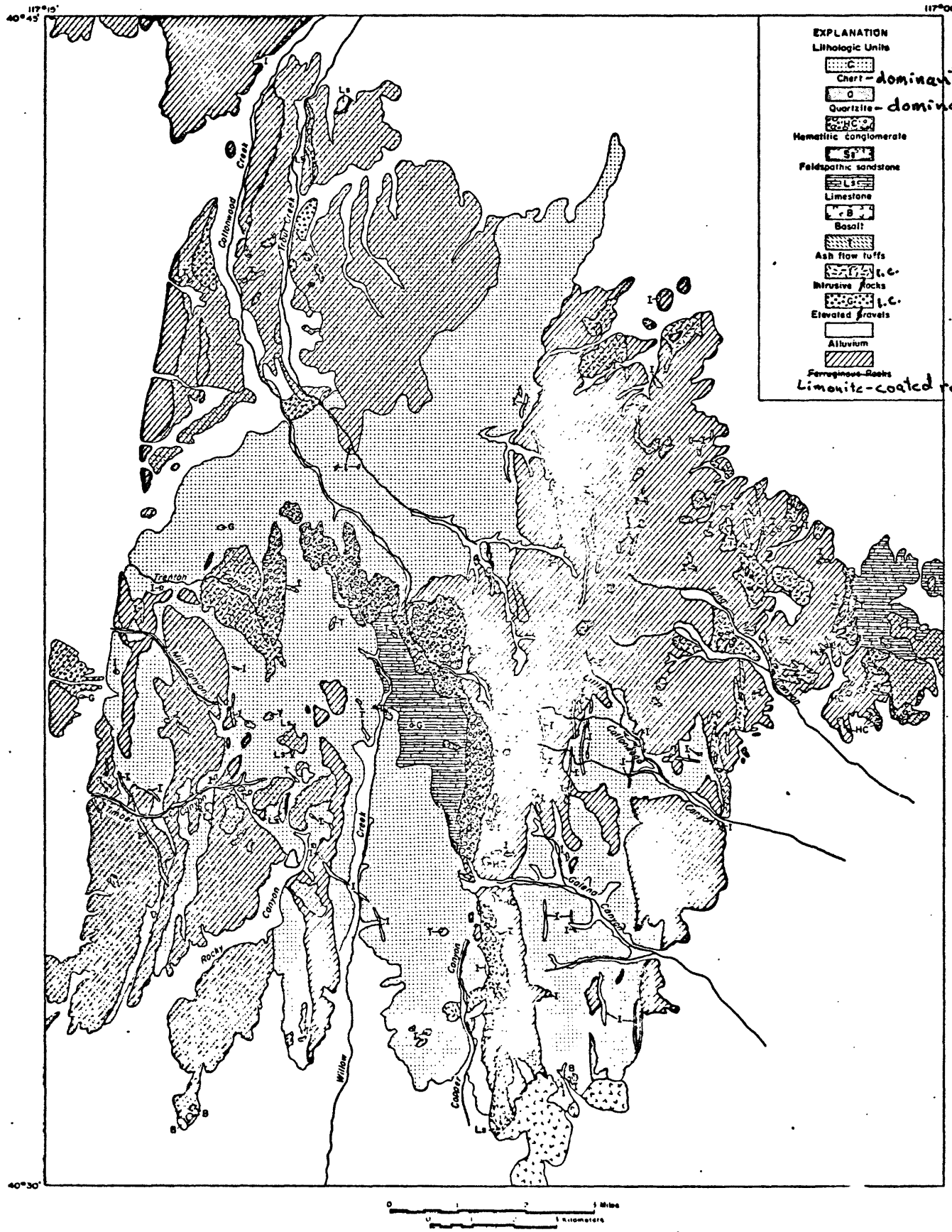
117°15'
117°00'
40°45'
40°30'
EXPLANATION
Lithologic Units
C
Chert – dominant
Q
Quartzite – dominant
HC
Hematitic conglomerate
Ss
Feldspathic sandstone
Ls
Limestone
B
Basalt
T
Ash flow tuffs
I.C.
Intrusive rocks
I.C.
Elevated gravels
Alluvium
Ferruginous Rocks
Limonite-coated rocks
Cottonwood Creek
Trenton Canyon
Mill Canyon
Rocky Canyon
Willow Creek
Cabin Canyon
Little Cottonwood Canyon
Colma Canyon
0
1
2
3 Miles
0
1
2
3 Kilometers

12A

and argillite. Quartzite, limestone, and sandstone are minor constituents. Some of the platy chert is fossiliferous, especially in the Pumpernickel formation. Limonite is common, and generally occurs on fracture surfaces as a bright reddish-yellow to dark brown stain.

Quartzite. Quartzite (unit Q, fig. 4) includes the quartzite member of the Valmy formation and the Mill Canyon member of the Havallah formation. Chert, dark shale, and greenstone are common minor constituents. Quartzite displays considerable variation in thickness, grain size, and composition of the matrix. In general, the albedo of the quartzite unit is higher than the chert unit. Pale reddish-brown limonite is visible on exposed surfaces and fractures in the quartzite. The quartzites of the Havallah formation tend to be thin-bedded, have calcareous cement, and are interbedded with limestone, whereas quartzites of the Valmy formation are thicker-bedded with silica cement.

Sandstone. The feldspathic sandstone unit (unit Ss, fig. 4) includes the Harmony formation and the Jory member of the Havallah formation. Composition varies from a feldspathic sandstone to an arkose, with grain size ranging from coarse sandstone to siltstone. Some calcareous cement is present. Minor interbedded components include shale, calcareous shale, limestone, and quartzite. Because of its mixed composition, the Harmony formation is highly susceptible to hydrothermal alteration. The alteration zone within the Harmony formation is larger than other units at Battle Mountain (Roberts and Arnold, 1965, p. B14).

Conglomerate. The Battle formation (unit HC, fig. 4) is a coarse, poorly-sorted, thick-bedded, chert-pebble conglomerate containing a characteristic medium to deep red silty hematitic matrix and some calcareous cement. As shown in figure 4, the conglomerate unit HC also includes a shale member and a dark colored chert-pebble and quartzite member.

Igneous Rocks

Most of the igneous rocks are younger than the widespread sedimentary cover present in the Battle Mountain area. The major exceptions are the Paleozoic greenstones that are interbedded with the chert and quartzite, especially in the Scott Canyon formation at Battle Mountain. Granitic intrusives between 153 m.y. and 87 m.y. old occur in the Buffalo Range, in the Tobin Range, in Trenton Canyon in Battle Mountain, and in Gold Acres (fig. 2) (Roberts and others, 1971; Theodore and others, 1973; Wrucke and Armbrustmacher, 1975; Stewart and Carlson, 1976). During a subsequent period of igneous activity, between 41 m.y. and 37 m.y. ago, numerous granitic bodies were emplaced throughout Battle Mountain, and also at Tenabo and at Granite Mountain in the Shoshone Range. (McKee and others, 1970) Many of the granitic bodies at Battle Mountain are thought to have been emplaced initially as granodiorites and subsequently altered to more potassium-rich rocks. Hydrothermal biotite at Copper Canyon yields K-Ar age dates essentially contemporaneous with the inferred emplacement ages of the adjacent granodiorite (Theodore and others, 1973).

The Cataeno tuff covers a large area of central Nevada, and is visible on Landsat images (Tc, fig. 3). The tuff is a vitric ash flow and water-lain rhyolitic tuff that crops out in a belt 97 km long and 9-22 km wide, south of Cortez, Nevada. The tuff contains abundant quartz phenocrysts in a light gray to pink groundmass that forms a deep reddish-brown limonitic weathering rind. Wrucke and Silberman (1975) dated the Cataeno tuff between 45 m.y. and 30 m.y. old, and proposed that the breccia pipes near Mt. Lewis in the Shoshone Range may be the source of the tuff. Silberman and others (1976) view the Cataeno as one of a series of stratiform rhyolitic and quartz latitic tuffs that blanketed central Nevada and eastern Utah between 34 m.y. and 17 m.y. ago. Basalt flows of late Tertiary and Quaternary age are scattered throughout Battle Mountain, the Shoshone Range, and the Fish Creek Range.

Limonite Coatings

Limonite is a general field term for a group of amorphous, naturally occurring ferric oxides and hydroxides. It includes the iron-bearing minerals goethite, hematite, jarosite, and lepidocrocite. In the Battle Mountain study area, limonite coatings on altered rocks appear to be derived primarily from the weathering of iron-sulfide minerals pyrite and pyrrhotite. Casts of remnant pyrite or pyrrhotite are common in the altered rocks.

Limonite coatings have a wide range of color and surface expression at Battle Mountain. Most of the coatings range in color

from light brown (5 YR 5/6) to moderate brown (5 YR 3/4). However, extreme colors from dark yellowish orange (10 YR 6/6) to blackish-red (5 YR 2/2) are present (Goddard and others, 1948). The limonite coatings commonly penetrate about 1 mm below the exposed surface, but coatings up to 3 mm were observed.

The surface expression of the limonite coatings is only relatively related to the bulk composition of iron in the rock. Igneous rocks generally contain more iron than the siliceous sedimentary rocks. Yet, limonite coatings commonly appear more conspicuous on light colored rocks, such as quartzite, than on dark colored rocks, such as greenstone, although the greenstone has considerably higher iron content than the quartzite (Gilluly and Gates, 1965, p. 12).

Limonite coatings are present on most altered rocks at Battle Mountain. However, some unaltered rocks have noticeable limonite coatings; unaltered chert and quartzite are problematic, especially when they are exposed on talus slopes. Also, some of the siltstone has a ferruginous matrix that is spectrally similar to the limonite. Changes between altered and unaltered rocks are subtle for the most part at Battle Mountain, and contacts between altered and unaltered rocks are commonly gradational.

Ore Deposits

A northwest-trending alignment of metal deposits in north-central Nevada over 400 km long has been termed the Battle Mountain-Eureka mineral belt, and includes deposits of gold, silver, lead, zinc,

copper, and tungsten (fig. 2) (Roberts, 1966; Horton, 1966). The belt is marked by a zone of north-northwest striking high-angle faults that transect the generally north-northeast-trending basin and range bounding faults, several Mesozoic and Tertiary granitic bodies, and is depicted in aeromagnetic maps (Shawe and others, 1976).

Two large porphyry copper systems dominate the mineral belt at Battle Mountain. (Sayers and others, 1968) Copper Basin (fig. 2) is a sulfide deposit that has undergone siliceous alteration, followed by extensive supergene enrichment; Copper Canyon is a hypogene replacement sulfide deposit that contains mostly potassic alteration assemblages with minor amounts of sericitic and argillic alteration. Other smaller vein-type mineral deposits are scattered across Battle Mountain.

In the Shoshone Range, over 15 base and precious metal deposits are located within a zone of geochemically anomalous metal concentration (Wrucke and Armbrustmacher, 1975). Antimony, tin, lead, and silver are present toward the northwest side of the zone; gold and tungsten are more abundant toward the southeast. Several ore deposits on the east side of the Shoshone Range, such as the Hilltop Bullion, Granite Mountain, and Tenabo deposits are located next to granitic bodies. An upper Cretaceous pluton is buried 120 m below ground at Gold Acres. Gold Acres lies at the extreme southeast margin of the geochemical zone along the Roberts Mountain thrust fault. Several other major disseminated gold deposits in north-central Nevada, such as Carlin and Cortez, are also situated on the Roberts Mountain thrust.

Hydrothermal Alteration

Copper Canyon. The hypogene replacement at Copper Canyon has undergone potassic, argillic, and some siliceous alteration. The lower chert pebble conglomerate of the Battle formation, the principal site of mineralization, has had its calcareous hematite-rich matrix replaced by an assemblage of hydrothermal potassic-feldspar, biotite, sphene, and sericite (Theodore and Blake, 1975). Adjacent host rocks, such as the Pumpernickel and Harmony formations, have had the siliceous components bleached and recrystallized, and the argillaceous components metamorphosed to biotite hornfels (Roberts and Theodore, 1971). In the ore bodies, sulfides are distributed in broad zones characterized by pyrite or pyrrhotite. Fault zones in the altered areas are generally intensely altered and lined with hydrous iron-oxides and clay minerals.

Copper Basin. The feldspathic and micaceous components of the Harmony formation are more susceptible to alteration than most other sedimentary units in Battle Mountain (Roberts and Arnold, 1965). The sandstones in the Harmony formation have been bleached and recrystallized, whereas the shaly rocks have been altered to purple-brown hornfels with fine specs of mica. Other alteration minerals include potassic-feldspar, epidote, zoisite, apatite, and biotite and white mica. The hornfels tend to weather into blocky rock fragments that form talus slopes on steep hillsides (Roberts and Arnold, 1965). Several other mining sites, such as Elder Creek (fig. 3) have similar types of alteration on a more restricted scale.

Gold Acres. The Gold Acres deposit is centered on a fenster of Paleozoic carbonate rocks exposed through the Roberts Mountain thrust. Chert, argillite, limestone, and greenstone surrounding the mine are altered to hornfels and calc-silicate rock and bleached almost white. Rocks near the open pit mine are intensely altered and locally kaolinized, and some limestone is weakly silicified. Quartz porphyry dikes intruded at the mine are thoroughly sericitized. The original sulfide minerals are largely oxidized to limonite, which is especially abundant along fault zones. The supergene processes that transported the iron is thought to have redistributed the other metals as well (Wrucke and Armbrustmacher, 1975, p. 6).

Table 2 presents a detailed comparison between Copper Canyon and Gold Acres. Both deposits contain submicroscopic gold, and have replacement minerals, but the deposits differ in age, host rock, and alteration history. The chief difference for this study is the limonite coatings of the altered rocks; limonite coatings are quite prevalent at Copper Canyon, but weak and not readily detectable on the bleached, altered rocks at Gold Acres. These two deposits may help to define constraints for mapping hydrothermal alteration from Multispectral Scanner images.

TABLE 2
Comparison of Alteration of Copper Canyon and Gold Acres

FACTOR	COPPER CANYON	GOLD ACRES
Type of Deposit	Hypogene replacement porphyry copper	Disseminated gold
Major Economic Metals	Cu, Au, Ag, Pb	Au, Ag
Controlling Structure	Virgin Fault	Roberts Mountain thrust & high-angle Cenozoic faults
Age	37.2 m.y.	92.8 m.y.
Pluton (Composition & Depth)	Altered quartz monzonite; exposed 152 m above surface	Granitic-buried 122 m below surface
Type of Alteration	Mainly potassic & argillic, with some skarn & sericitic	Argillic & siliceous
Major Sulfide Minerals	Pyrite, pyrrhotite (oxidized to limonite), chalcopyrite, arsenopyrite, marcasite	Pyrite (oxidized to limonite), sphalerite, pyrrhotite, marcasite
Host Rocks	Sandstone & shale (Harmony fm), hematitic conglomerate (Battle fm), chert (Pumpernickel & Scott Canyon fm)	Chert, argillite & greenstone (Valmy fm), limestone
Iron-Oxide Minerals	Extensive limonite surficial coating on altered cherts & sandstone; also found intensified in fault & fracture zones	Altered siliceous rocks bleached but relatively lacking in limonite; iron-oxide minerals concentrated along fault zones
Alteration Products	Skarn, potassium, feldspar, hydrothermal biotite	Hornfels, tactite, kaolinite, hexahydrite
Ore Deposition Stages	Early-310-360°C: Cu, FeS, Mo, K-spar Middle-325°C: Pb, Zn, Fes, FeS_2, $FeCO_3$ Late-225°C: Au, Quartz (Theodore & Blake, 1975, p. B52)	Early-380°C: Mo, W Middle-260°C: Zn, Cu, Mn Late-150-250°C: Au, As, B, Hg, W (Hot Springs) (Wrucke & Armbrustmacher, 1975, p. 24)
Depth of Oxidation	60-90 m	60-120 m

DESCRIPTION OF IMAGES AND PHOTOGRAPHS

Eight types of image products (table 3) were evaluated for their potential for mapping hydrothermally altered rocks in the study area. The color-ratio composite was the principal product used to discriminate hydrothermal alteration and several images from different playback devices with various scales and qualities of resolution (#2, 3, 5, table 3) were produced. Due to the degradation of topographic and cultural features inherent to ratio processing, other types of images and aerial photographs were needed to determine the exact field location of areas in the CRC. The following section briefly describes the new procedures used for making and evaluating the CRC images.

Color-ratio composite images (CRC) portray spectral radiance variation because brightness variations due to topographic slope and albedo are subdued by ratioing the spatially registered digital numbers (DN) of two MSS bands (Rowan and others, 1974; Goetz and others, 1975). The ratio values are played back as a black-and-white image on a digital-to-analog film recorder. Because the ratios span only a small part of the total numerical range of the film recorder (0-255), a contrast stretch algorithm is used to take advantage of the complete range. Several stretching algorithms are available, but a linear stretch has proven most useful in the study area. The film recording convention adopted portrays low ratio values as dark pixels and high ratio values as light pixels.

Table 3

Summary of Images and Photographs Used in Alteration Mapping of Battle Mountain-Eureka Mineral Belt

TYPE OF PRODUCT	SCALE	FORMAT	SCENE ID#, ACQUI. DATE	FIG#	COMMENTS
1. Landsat color-infrared composite	1:1,000,000	17.7 cm x 18.5 cm color print & transparency	1397-17590, 23 Aug 73 (044-032) - EROS Data Center ID # for 2nd edition of selected Landsat images for the conterminous U.S.	3	Used with CRC for field location of altered areas. Some bleached altered areas appear bright, but many unaltered areas also have high albedo.
2. 70 mm Landsat color-ratio composite (Video Film Converter playback)	1:3,375,000 enlarged to 1:250,000	55.8 mm diazo composite enlarged to 74.5 cm color print	1054-17592, 15 Sept 72 Sun elevation 46° Sun azimuth 141°		Distortion & loss of resolution due to 13.2x enlargement. Spherical distortion 0.643%. Print is red saturated in vegetated areas with blue cast in alluvium. Landmarks and streams are fuzzy.
3. Large format Landsat color-ratio composite (Geospace 34/10 playback)	1:325,000	64 cm x 61 cm diazo composite contact printed onto Cibachrome Stretches 2% linear - 4/5,4/6,5/6 6% linear - 6/7	1054-17592, 15 Sept72	5 6	Distortion less than .027 cm over frame; Landsat pixel size 265x254 µm played out at machine scale of 96 pixels/inch. Cultural and drainage landmarks one pixel wide are visible. Registration of diazo composites is limited to approx. 1/4 of frame and is good to within 1/4 of a pixel.
4. Large format Landsat band 5 (Geospace 34/10 playback)	1:325,000 enlarged to 1:250,000	64 cm x 61.6 cm black-and-white transparency	1054-17592, 15 Sept72	7	Linear stretch. Used to provide accurate location for altered areas in CRC. Film density range is 0.25 to 1.65.
5. Digital enlargement of Battle Mountain range (Optronics P-1700 playback)	1:200,000	16 cm x 17 cm diazo composite contact printed onto Cibachrome	1054-17592, 15 Sept72	8	Pixel size 400 µm. Wide digital enlargement Each 100 µ pixel replicated 16 x into a 4x4 matrix. Misregistration of ratio images is about 1/4 pixel. Sharp square pixels.
6. Skylab S-190A	1:1,019,000	16 cm x 16 cm color print	SL3, roll 28, frames 186-187, 12 Aug 73		Color balance of print highly monochromatic. Altered areas cannot be discriminated. No stereo overlap.
7. High-altitude color & color-infrared photography	1:95,000	22.7 cm x 22.7 cm color transparency & prints	NASA Johnson Space Center, Mission 310, rolls 7&8, 13 May 75		Mountain peaks snow covered; widespread vegetation cover visible in infrared. Slight reddish cast visible on forward half of all frames
	1:122,700	22.7 cm x 22.7 cm color transparency & prints	Ames U-2 flight 75-171 10 Oct 75	10	Photography used extensively for field location. Bluish cast hinders discerning bleached areas on color & vegetation on CIR. Talus slopes of altered rocks discernible.
8. Low-altitude color photography	1:36,300	23 cm x 23 cm color transparency	NASA Johnson Space Center, Mission 340, June 76		Good resolution, but restricted to Gold Acres area; brownish cast impedes rock type discrimination

To form a color-ratio composite, two or three stretched black-and-white positive ratio images are combined using different color diazo film or color filters. In this study, diazo film is used because of its high contrast and because of the amount of control it allows the operator in bringing out subtle color variations. Diazo film is an ammonia-based positive-to-positve film such that increased exposure lightens or burns out more of the original. Three diazo separates are registered together to form a single composite image with subtractive colors.

Several changes have been instituted to improve the black-and-white film recording and color compositing of the ratio images. Previous studies (Rowan and others, 1974, 1977) used 70 mm black-and-white ratio images played back on a Video Film Converter (VFC) at the Jet Propulsion Laboratory. These images were color-composited and enlarged to 1:500,000 or 1:250,000 scale color prints. Spherical lens distortion in the enlarged print produced from the 70 mm CRC measured 2.5 mm in 325 mm.

The new approach utilizes the Geospace 34/10 plotter for generating large format black-and-white images up to 83 cm square. Three pixel writing sizes are available, 48, 96, and 192 pixels per inch (0.259, 0.265, and 0.133 mm/pixel), with a stated precision of $\pm$.005 in. (0.013 cm) across the diagonal. For the Battle Mountain-Eureka scene, the entire scene was played back at 96 pixels per inch, resulting in a 63 cm x 61.6 cm image, with a pixel size of 265 x 254 microns.

The chief advantage of large format ratio images is that they can be registered more precisely than was previously possible with the 70 mm images. However, the diazo material is not stable over the entire image. Therefore, individual color-ratio composite images for the study area are limited to no more than approximately 1/4 of the scene. Internal registration of these 1/4 frame images is estimated to be within about 1/4 of a pixel. Using the large format CRC images, stream canyons can be located as lines of vegetation only one pixel wide, and small vein-type altered areas of only two to three pixels that were previously indistinguishable in the 70 mm products can be discerned.

Selection of Ratios

The selection of MSS ratio images used to form color-ratio composite images is based both on known spectral reflectances of rock and vegetation types in the MSS response range, and on visual evaluation of the images. The approximate MSS bandpasses are 0.5 μm-0.6 μm Band 4, 0.6 μm-0.7 μm Band 5, 0.7 μm-0.8 μm Band 6, and 0.8 μm-1.1 μm Band 7. In the south-central Nevada study area, the optimum composite was made using MSS 4/5 as blue, MSS 5/6 as yellow, and MSS 6/7 as magenta (Rowan and others, 1974). With such a diazo color scheme and film density convention, limonitic areas appear green to green-brown in the CRC image; felsic rocks are orange-pink to brown-pink; mafic rocks, some sedimentary rocks, and cloud shadows are white; playas are blue; and vegetation is orange.

A color-ratio composite image for the Battle Mountain-Eureka scene using this combination of MSS ratio images and diazo colors (fig. 5) shows most large areas of limonitic hydrothermally altered rocks, such as the Long Peak-Copper Basin area (A, fig. 5) and Copper Canyon (B, fig. 5) (Roberts and Arnold, 1965) as diffuse green areas. The green hues in the CRC (fig. 5) correspond to 2.5 BG 5/2 - 7.5 G 5/4 in the Munsell notation (Munsell Color Co., 1969). However, the limonitic altered area east of Long Peak (C, fig. 5) is indistinct, and the Copper Canyon deposit (B, fig. 5) appears predominantly blue, with only a few interspersed patches of green. Moreover, reference features are poorly defined in this CRC image.

The loss of discrimination of limonitic rocks in the 5/6 CRC image (fig. 5) is apparently caused by the vegetation density in the Battle Mountain-Eureka area. In general, the ratios of vegetation are lower than limonite in both MSS 5/6 and MSS 4/6 because of the steeper rise of vegetation reflectance from the visible to near-infrared region (Knipling, 1970). Where vegetation is sparse, such as in south-central Nevada, moderately severe contrast stretching results in saturated black pixels for vegetation, and moderately dark gray pixels representing limonite. As vegetation density increases, more severe stretches are needed to translate the limonite pixels to gray tones that can be portrayed in the yellow diazo separates. However, severe stretching of MSS 5/6 ratio images is not feasible owing to its low signal-to-noise characteristics (Siegal and Goetz, 1977). The relatively high

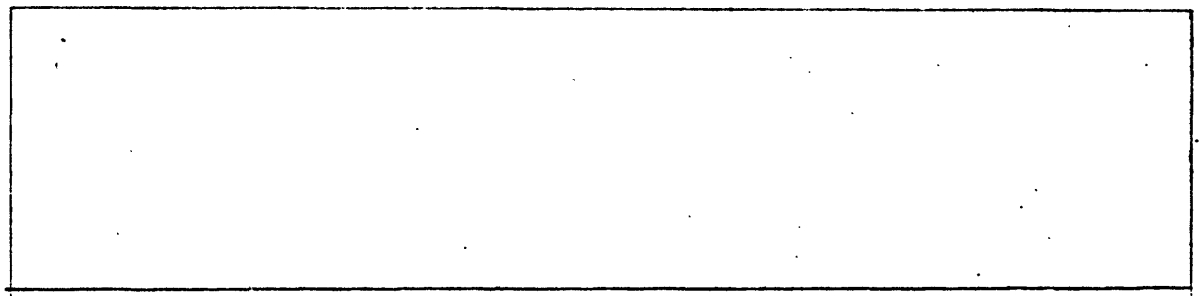

Figure 5 - Large format color-ratio composite image of part of the Battle Mountain-Eureka mineral belt, with MSS 4/5 as blue, MSS 5/6 as yellow, and MSS 6/7 as magenta (see oversized images).

contrast of the MSS 4/6 images permits more severe stretching without producing unacceptably noisy images, and hence increases enhancement of limonitic areas.

The increased color definition of the limonitic areas is apparent in the color-ratio composite, in which MSS 4/6 replaces MSS 5/6 as the yellow layer (fig. 6). The green hues in the CRC with MSS 4/6 correspond to 2.5 GY 5/4 - 2.5 GY 6/6 of the Munsell notation (Munsell Color Co., 1969). Resolution of the alteration zone at Copper Basin (A, fig. 6) is much improved, and alteration at Copper Canyon (B, fig. 6) is also detectable, whereas in figure 8, the alteration is indistinct. The increased discrimination of limonite is evident in unaltered limonitic rocks as well. The belt of Cataeno tuff (Tc, fig. 6) is a distinct green on the CRC image, whereas on the MSS 5/6 CRC image (fig. 5), it is more blue. Limonitic alluvium is also more noticeable in figure 6 than in figure 5.

The second major difference between the two CRCs is the portrayal of vegetation. Much of the shrub vegetation appears yellow in the MSS 5/6 CRC image (fig. 5). In the MSS 4/6 color-ratio composite (fig. 6), vegetation is predominantly red, indicating the MSS 6/7 ratio component. Thus, due to the higher vegetation density at Battle Mountain, the use of MSS 4/6 is needed to increase the discrimination of limonite. However, the unaltered limonitic rocks are also more evident.

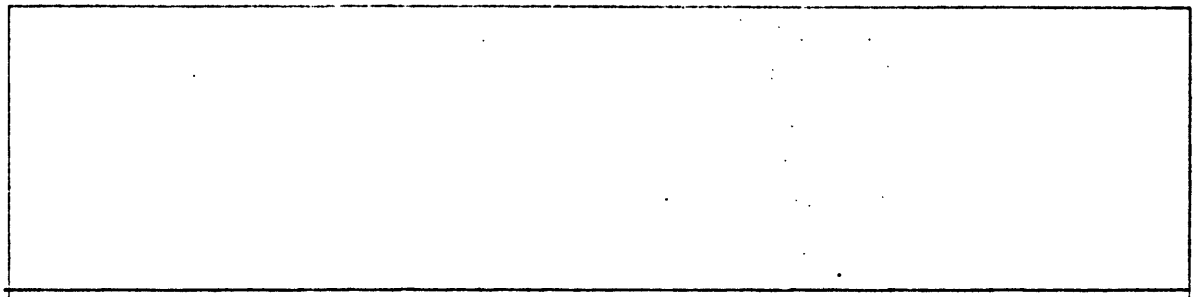

Figure 6 - Large-format color-ratio composite image of part of the Battle Mountain-Eureka mineral belt, with MSS 4/5 as blue, MSS 4/6 as yellow, and MSS 6/7 as magenta. A, Copper Basin mine; B, Copper Canyon mine; C, Hilltop mining district; D, Bullion mining district; E, Gold Acres mine; F, Tenabo mining district; G, altered Slaven chert with turquoise mine; H, unaltered limonitic Valmy quartzite; I, altered andesitic basalt at Fire Creek; J, breccia pipe in Horse Canyon; K, Maysville Canyon; Tc, Cataeno tuff (see oversized images).

Color Extraction

The subjectivity and associated imprecision of the earlier visual delineation of colors has been eliminated in this study by using a color recognition drum scanner for extracting green pixels from the CRC image. The scanner being used is a Linoscan Color Scanner, Model #204/6, located at E.I. DuPont de Nemours and Company, Inc., Bethel, Pennsylvania. Cibachrome prints of the CRC images were scanned because misregistration of the diazo separates resulted when the original composite was wrapped around the drum. Resolution of the scanner can be set at 500 or 1000 lines per inch (197 or 394 lines/cm). A high contrast black-and-white film copy, showing the distribution of the extracted color, is exposed during the scan. Time for a complete scan, including film development, is approximately 20 minutes for a 8"x10" image.

Color extraction is based on recognition of specified colors taken from the image. The selected spot of color, approximately 0.5 mm in diameter, is separated into cyan, yellow, magenta, and a brightness component. The tricolorimetric color components are displayed as digital numbers, which are relative, and are not related to optical wavelengths. The user can set a range around the tricolorimetric numbers; the wider the range, the more color shades are included in the extraction. Up to six input color channels can be used during one scan.

A set of color extractions was made on the Battle Mountain-Eureka CRC image (fig. 7). The blue areas on the extracted image represent

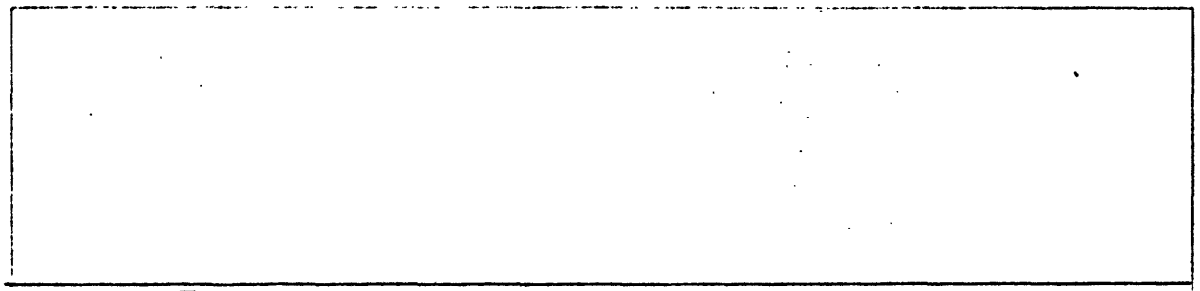

Figure -7- Linoscan color separation of green hues from MSS 4/6 color-ratio composite superimposed on an MSS band 5 image. Dark blue is the dark green color extraction; yellow is the light green color extraction (see oversized images) (see fig. 6 for localities).

the darker greens of the CRC image, and the yellow areas include more of the lighter green hues. The different separates were made by using a different set of reference pixels. The separation illustrates how much more of the greens are depicted if the lighter hues are used. Use of machine color extraction makes it possible to produce an objective limonitic materials map from the CRC image. Additional steps are needed to eliminate areas of limonitic unaltered rocks and produce a map of limonitic hydrothermal alteration. Of the four study areas in the Great Basin, the Battle Mountain study area contains the largest area of limonitic rocks that are unaltered.

EVALUATION OF THE COLOR-RATIO COMPOSITE IMAGE

Examination of the MSS 4/6 CRC image (fig. 6) reveals that green pixels depict unaltered, as well as altered, limonitic rocks. These pixels range from dark to light green, presumably due to variation in the amount of limonite present on the surface of the rocks. The color extraction (fig. 7) illustrates the problem in this study area of defining what threshold of green hues to include in an alteration map. The lighter green pixels (yellow, fig. 7) furnish a more complete representation of altered areas than the darker green pixels alone (blue, fig. 7), but many more of the unaltered limonitic rocks are included in the yellow pattern.

Unaltered limonitic rocks depicted in the CRC image (fig. 6) are of sedimentary and volcanic origin. The sedimentary rocks include sandstone and siltstone of the Havallah formation and the quartzite member of the Valmy formation. Limonitic volcanic rocks include the Tertiary Cataeno tuff and an unnamed Tertiary andesitic basalt occurring mostly in the western half of figure 6. A detailed discussion of the composition and the spectral characteristics of both the altered and unaltered limonitic rocks is presented below for Battle Mountain and the Shoshone Range.

Battle Mountain

A digital enlargement of the CRC image for the Battle Mountain area (fig. 8) was produced by replicating each pixel 16 times into a 4x4 matrix (table 3, no. 5). Each pixel is 400 microns on a side, and a smoothing function has been applied to avoid a blocky appearance. Alteration halos of the two major copper porphyry deposits, Copper Canyon and Copper Basin, are readily apparent in this CRC image (figs. 8 and 9). The large green area southeast of Copper Basin represents limonitic alluvial deposits derived as fanglomeratic debris from Long Canyon. Thus, as in south-central Nevada (Rowan and others, 1974), the CRC mapping technique must be restricted to areas of outcrop. Other altered areas visible in the CRC image are the prospects and mines around Elder Creek, located 6.5 km northwest of Copper Basin, and the altered area associated with a granodiorite at Trenton Canyon on the western side of the range (fig. 9). In both cases, the country rock surrounding the granitic bodies has been bleached and recrystallized, thereby yielding a rust-brown limonitic coating. In general, however, the differences between altered and unaltered rocks are not distinct. Sedimentary host rocks are dark, and limonite does not form a conspicuous coating. Rather, the differences between altered and unaltered rocks are gradational, and thus definition of the alteration boundary is commonly imprecise.

Several smaller mines associated with vein-type deposits are visible as a few green pixels in the digital enlargement (fig. 9). These include the DeWitt mine, the Antimony King mine, some of the

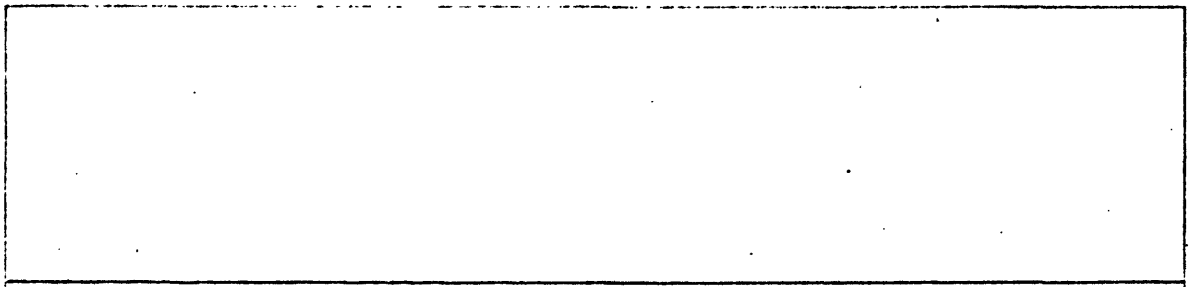

Figure 8 Digital enlargement of the color-ratio composite image for the Battle Mountain range. MSS 4/5 is blue, MSS 4/6 is yellow, and MSS 6/7 is magenta. Each Landsat pixel consists of 16 playback pixels in a 4x4 matrix. Sites A are the west-facing hillslopes of altered Harmony formation that appear white because of topographic effects. The white area at B is a non-limonitic type of alteration.

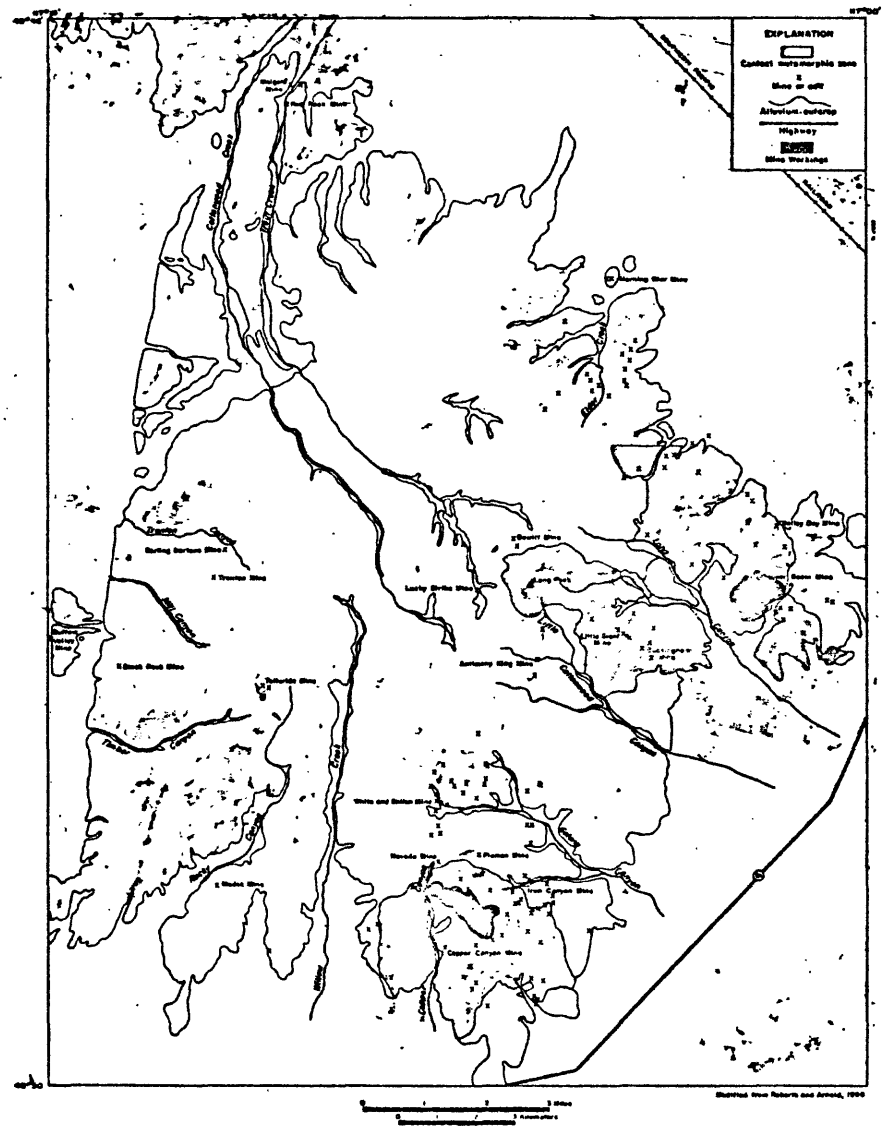

ALTERATION MAP OF ANTLER PEAK 15' QUADRANGLE

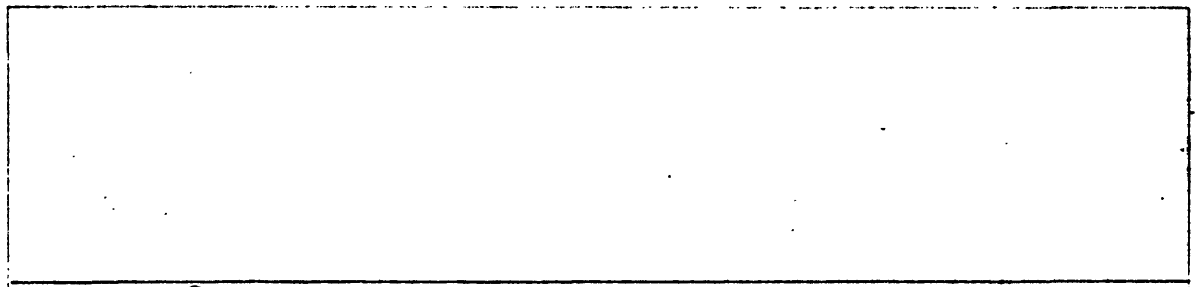

Figure 9 Linoscan color separation of the green hues (shown in red) from the digital enlargement of the Battle Mountain Range (fig. 8), superimposed on an alteration map of the Antler Peak 15' quadrangle (after Roberts and Arnold, 1965).

Galena Canyon mines, the Telluride mine, the Buffalo Valley mine, and the Marigold mine (fig. 9). The surface expression of the vein deposits varies from highly bleached chert beds of the Havallah formation at the Buffalo Valley mine to the slightly silicified drab hornfels of the Harmony formation at the DeWitt mine.

The CRC composite (fig. 8) is particularly effective in discriminating the large altered zone of the supergene Copper Basin deposit. Most of the limonitic altered rocks in this zone are also visible as a subtle red hue on high-altitude color aerial photographs (A, fig. 10). The talus slopes of the silicified Harmony formation near Long Peak (B, fig. 10) are apparent due to the presence of dark brownish-black limonite coating. However, many limonitic altered areas are obscured in the photographs, both by shadows and the blue hue that is typical of all these color aerial photographs. Unaltered rocks, such as the Antler Peak limestone (C, fig. 10) appear pink in the photograph, whereas they appear white in the CRC (fig. 8), indicative of non-limonitic rocks.

Comparison of the limonitic areas from the CRC image (fig. 9) to the lithologic map of Battle Mountain (fig. 4) shows that several areas of unaltered limonitic rocks are depicted by the image. The two largest areas are the quartzite in the vicinity of Timber and Rocky Canyons, and the feldspathic sandstone near the northern portion of Cottonwood Creek. In the field, the limonite coatings of these rocks are readily apparent. However, many other unaltered rocks also have some form of limonite coating as interpreted in the lithologic

map (fig. 4). In an area with widespread limonitic coatings over the rock, the CRC can still distinguish unaltered rocks from most altered rocks. The [amount] presence of unaltered limonitic rocks, however, is a limitation on using the CRC for mapping hydrothermal alteration.

Topographic Effects

A few areas within the Copper Basin limonitic alteration zone appear white rather than green in the CRC image (fig. 8). The largest white areas trend northeast through the Little Giant mine area (A, fig. 8) along the southwestern edge of the alteration halo and north of the pit at Copper Basin (B, fig. 8). These areas correspond to northwest-facing hill slopes of limonitic altered rocks.

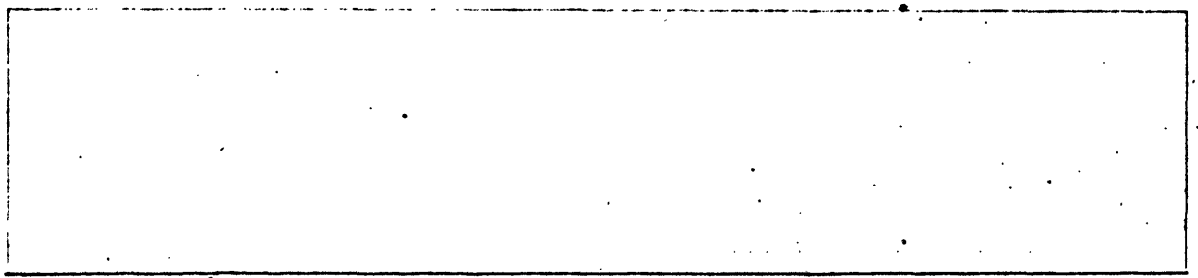

Figure 10 - High-altitude U-2 color aerial photograph of the Copper Basin mine and surrounding area. A is the Duval open pit. B is the talus slopes of dark limonite-coated altered Harmony formation at Long Peak. C is the unaltered Antler Peak limestone that appears red in the photograph.

The dips of these slopes are as low as 20 degrees, although they have a wide azimuthal range (fig. 11). Solar orientation at the time of acquisition of this scene was 141 degrees azimuth and 46 degrees elevation (A, fig. 11). Thus, penumbral shadows only occur on slopes greater than 46 degrees (B, fig. 11). The presence of white areas on slopes as low as 20 degrees appears to be due to low radiance levels and atmospheric scattering. Atmospheric scattering is greater in the short wavelength than long wavelength MSS bands, and is especially important in MSS band 4. For example, estimates of the scattering contribution in the MSS bands for the Goldfield, Nevada scene are 24, 10, 6, and 1 for MSS 4, 5, 6, and 7, respectively; for the atmospheric correction, these digital numbers were subtracted from the original MSS data transformed between 0-255 (Goetz and others, 1975). This technique is known as dark object subtraction. Thus, the MSS 4 radiance recorded by the MSS from dark surfaces is in large part scattered light. Consequently, ratios having MSS 4 in the numerator will be abnormally high, and in the case of limonitic rocks on shaded slopes, MSS 4/5 and 4/6 may be so large that the representative pixels appear white instead of blue and yellow, respectively, as depicted in figure 8.

A second white area northwest of the pit at Copper Basin (B, fig. 8) is due to the presence of non-limonitic altered rocks rather than topographic effects. Most of these rocks are pale to dark green coarse-grained sedimentary and dark brownish-purple fine-grained shales. Limonite is generally lacking.

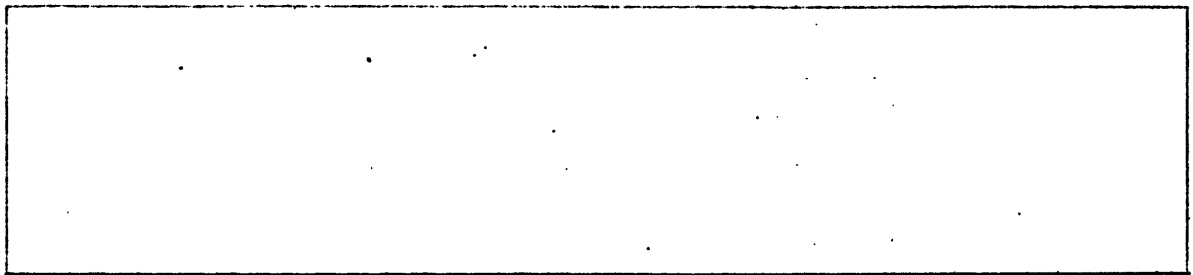

Figure 11 - Lower hemisphere stereographic projection of poles to slope of altered hillsides depicted as white in the CRC image of Battle Mountain (fig. 8). Slopes were measured in the field looking down from the inflection point of the hillside (Hack and Goodlett, 1960, p. 10). A, sunline at image acquisition (azimuth 141°, elevation 46°); B, hemisphere of penumbral shadow C, hemisphere of sunlight. All the slopes measured in the field at white areas in the CRC image have dips less than those required for penumbral shadow, suggesting that effects, such as low radiance levels or atmospheric scattering, are being observed in the CRC image.

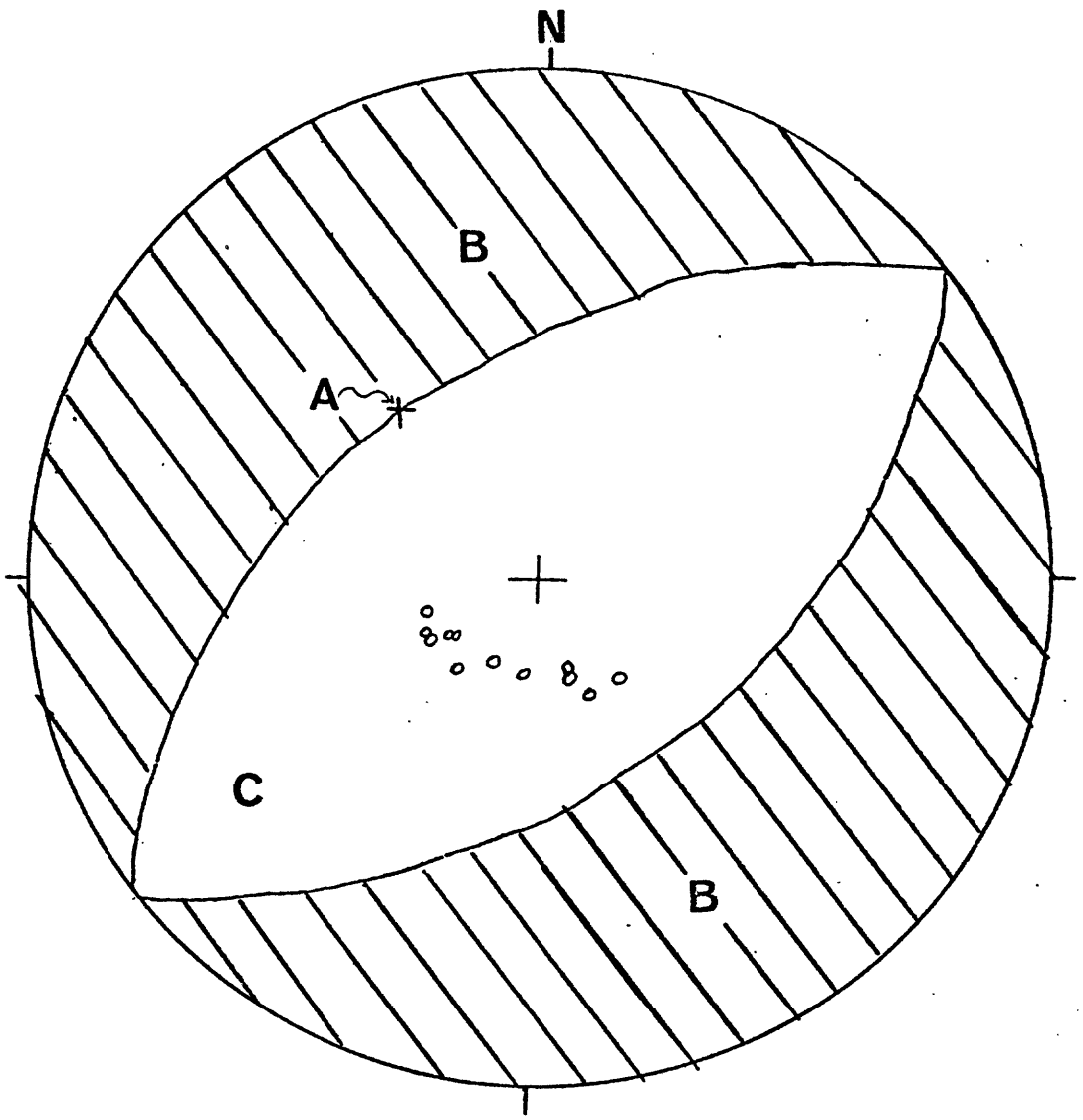

o - Values of poles to slope measured at Battle Mountain.

white areas within the alteration pattern depicted in the CRC may be caused by lithologic, as well as slope effects, and therefore must be interpreted with caution.

An atmospheric correction was applied to the ratio images of the Battle Mountain area using the technique of dark object subtraction (Abrams, written comm., 1977). Preliminary examination of the CRC image with atmospheric correction shows that altered areas with known west-facing topographic slope, such as the Little Giant mine area (A, fig. 8) are correctly represented as limonitic areas in the image. Other altered areas, such as the Copper Canyon mine, show a better fit to the mapped contact metamorphic zone. Furthermore, the area of non-limonitic alteration northwest of Copper Basin (B, fig. 8) is still essentially white in the corrected CRC image. However, the atmospheric correction does cause some side effects; the corrected CRC image is generally noisier, has more non-altered limonitic areas, and shows more brown areas in the vegetated mountain areas than the uncorrected CRC image. Because of these complications, a more detailed analysis is needed before specific comparisons can be made between the CRC images with and without atmospheric corrections.

In Situ Spectra

A reflectance spectrum of a specimen of altered bleached Harmony formation at Copper Basin (A and B, fig. 12) recorded in the field using the Portable Field Reflectance Spectrometer (PFRS) (Goetz and others, 1975), illustrates the characteristic ferric iron absorption features that allow discrimination of limonite in the CRC image. The steep slope of the reflectance curve between 0.4 μm and 0.7 μm is a combination of a charge-transfer absorption band centered in the ultraviolet and several less intense absorption bands between 0.4 μm and 0.6 μm due to crystal field transitions (Hunt, 1977). The steep slope of the reflectance curve means that MSS band 4 will be depressed with respect to MSS band 5 and MSS band 6, resulting in a low value for the MSS 4/5 and MSS 4/6 ratios. Another intense crystal field transition band related to ferric ions is centered at 0.87 μm (Hunt and others, 1971) (A and B, fig. 12). The reflectance in MSS band 7 is less than or equal to MSS band 6, resulting in a high MSS 6/7 ratio value.

The in situ reflectance spectra of the altered Harmony quartzite and argillite (fig. 12) also show that an absorption band is present in the 2.2 μm-2.3 μm wavelength region. Absorption bands in the longer wavelengths result from vibrational processes rather than crystal field transitions, as in the iron absorption bands. The 2.2 μm band is a combination band of the fundamental O-H stretching mode, and is observed in the spectra of clay minerals, amphiboles, and some micas (Hunt, 1977). Laboratory reflectance spectra (fig. 13)

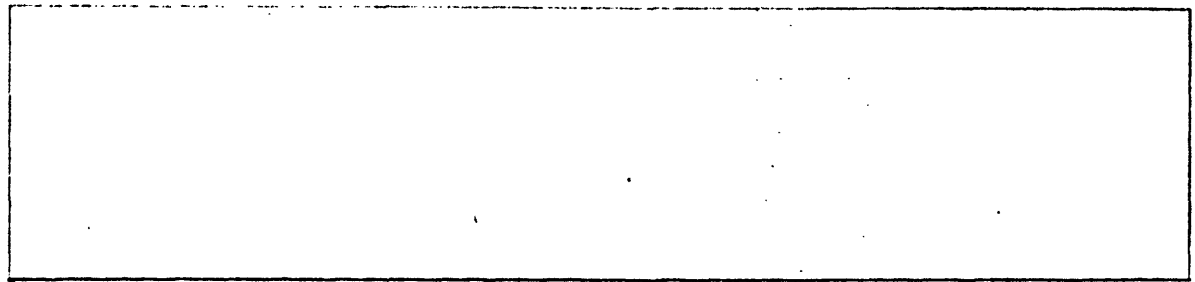

Figure 12 - *In situ* reflectance spectra of specimens of the altered Harmony formation from the vicinity of Copper Basin. A, spectrum of quartzite fragments with 2 percent dried grass vegetation. Note the slight absorption band at 2.1 μm indicative of vegetation. B, mixture of quartzite and argillite.

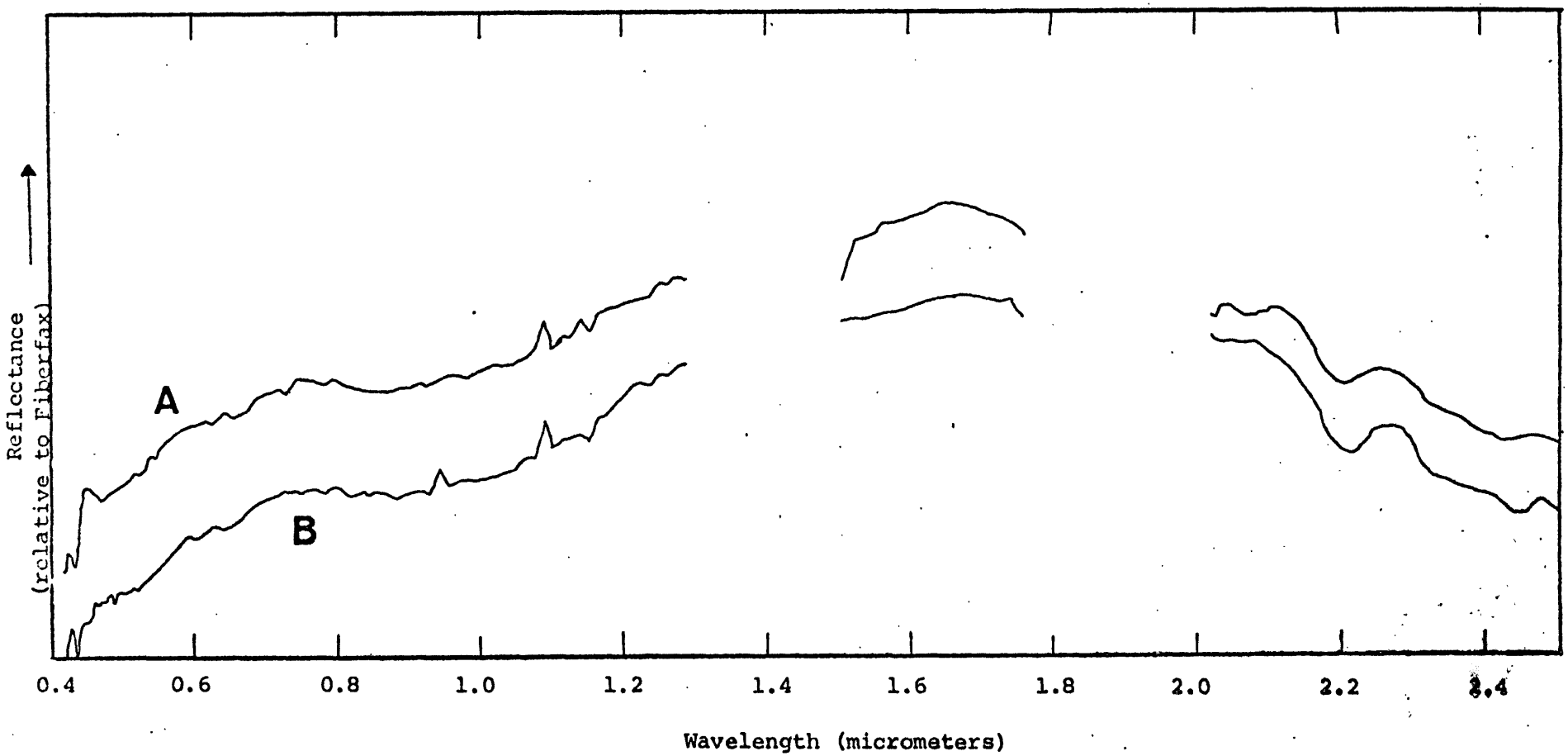
Reflectance
(relative to Fiberfax)
A
B
0.4
0.6
0.8
1.0
1.2
1.4
1.6
1.8
2.0
2.2
2.4
Wavelength (micrometers)

Figure 12

13

Figure - Laboratory reflectance spectra of specimens of altered and unaltered Harmony formation. Samples were collected adjacent to a vein of hydrothermally altered rock at the mouth of Cottonwood Canyon, south of the Copper Basin mine (fig. 9). Note that the absorption band near 2.2 μm is present in the spectrum of altered rock, but is weakly expressed in the spectrum of the unaltered rock.

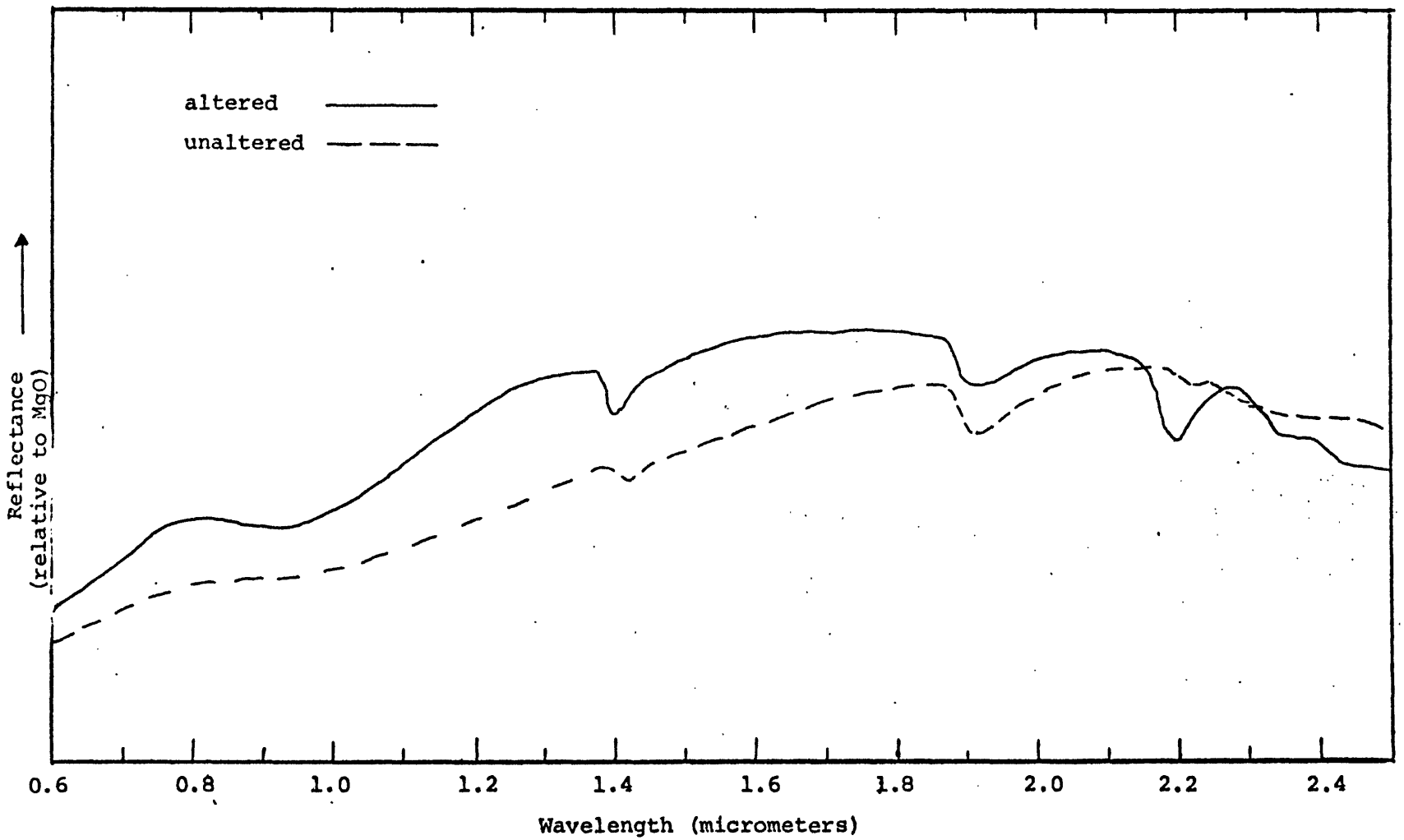
altered
unaltered
Reflectance
(relative to MgO)
0.6
0.8
1.0
1.2
1.4
1.6
1.8
2.0
2.2
2.4
Wavelength (micrometers)

Figure 13

of samples of the Harmony formation collected near the south margin of the contact metamorphic zone of Copper Basin (fig. 9), show that the 2.2 μm absorption band is present in the altered sample, but absent in adjacent rocks that are unaltered. In this area, limonite by itself appears insufficient in this area to discriminate altered from unaltered rocks consistently.

The exact position of the absorption band at 2.2 μm is related to the coordination and molecular position of the hydroxyl group. Minerals with Al-OH bonds, such as kaolinite, have absorption bands at 2.20 μm, whereas minerals with Mg-OH bonds have the absorption band shifted toward 2.3 μm. For example, the absorption band for montmorillonite is centered near 2.22 μm (Hunt and others, 1973). Laboratory experiments with mixtures of kaolinite and montmorillonite have shown that the absorption bands at 2.20 μm and 2.22 μm shift proportional to the mixture composition of the end members.

The altered Harmony quartzite spectrum (A, fig. 12) has an absorption minimum at 2.20 μm, whereas the altered Harmony argillite spectrum (B, fig. 12) has the band shifted toward 2.22 μm. X-ray diffraction shows that kaolinite is the only clay mineral in both samples; however, the X-rays also indicate that K-mica is present in the argillite. Muscovite has an absorption band at 2.22 μm (Hunt and Salisbury, 1970). Thus, the shift in the 2.2 μm band of the Harmony argillite spectrum (B, fig. 12) appears to be caused by K-mica rather than montmorillonite.

Due to the limited number of field spectra, few conclusions can be made about the spectral characteristics of the altered Harmony formation, but the successful discrimination of the altered zone in the CRC image indicates that most of the altered rocks are characterized by intense ferric iron absorption. In addition, the field spectra indicate that differences in the alteration pattern might be remotely discriminated using wavelengths between 1.1 μm and 2.5 μm.

Copper Canyon

The alteration halo surrounding the Copper Canyon deposit is also visible in the CRC image, although it is more restricted than the halo at Copper Basin. The halo is predominantly underlain by chert of the Pumpernickel formation to the west, and of the Scott Canyon formation to the east (Roberts, 1964). The Battle formation, a hematitic conglomerate that is the principal productive sedimentary unit at Copper Canyon, has been largely obscured by the mine workings; it is visible as the blue and white areas in the CRC (fig. 6). Other white areas in the halo represent topographic effects. The chert of the Pumpernickel and Scott Canyon formations, normally dark blue or brown in color, is extensively bleached to a light tan or white within the alteration halo. Tan to dark brown limonite coatings occur extensively over the exposed rock surface. These coatings are commonly much lighter than the limonite coatings on the talus slopes of the Harmony formation. Laboratory reflectance spectra (fig. 14)

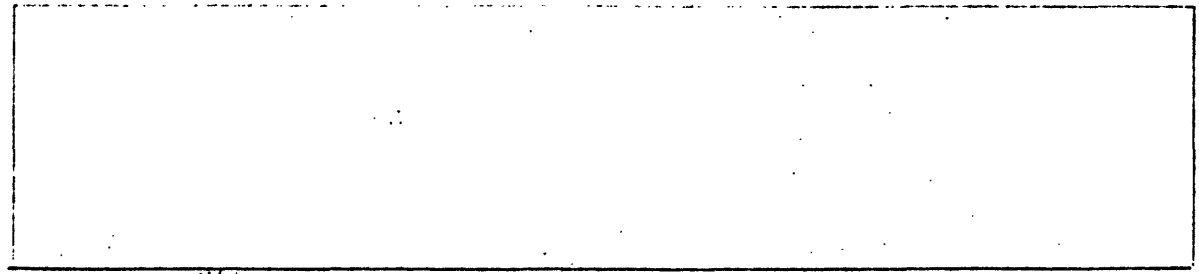

Figure 14 - Laboratory reflectance spectra of specimens of altered and unaltered chert of the Scott Canyon formation from the vicinity of Copper Canyon.

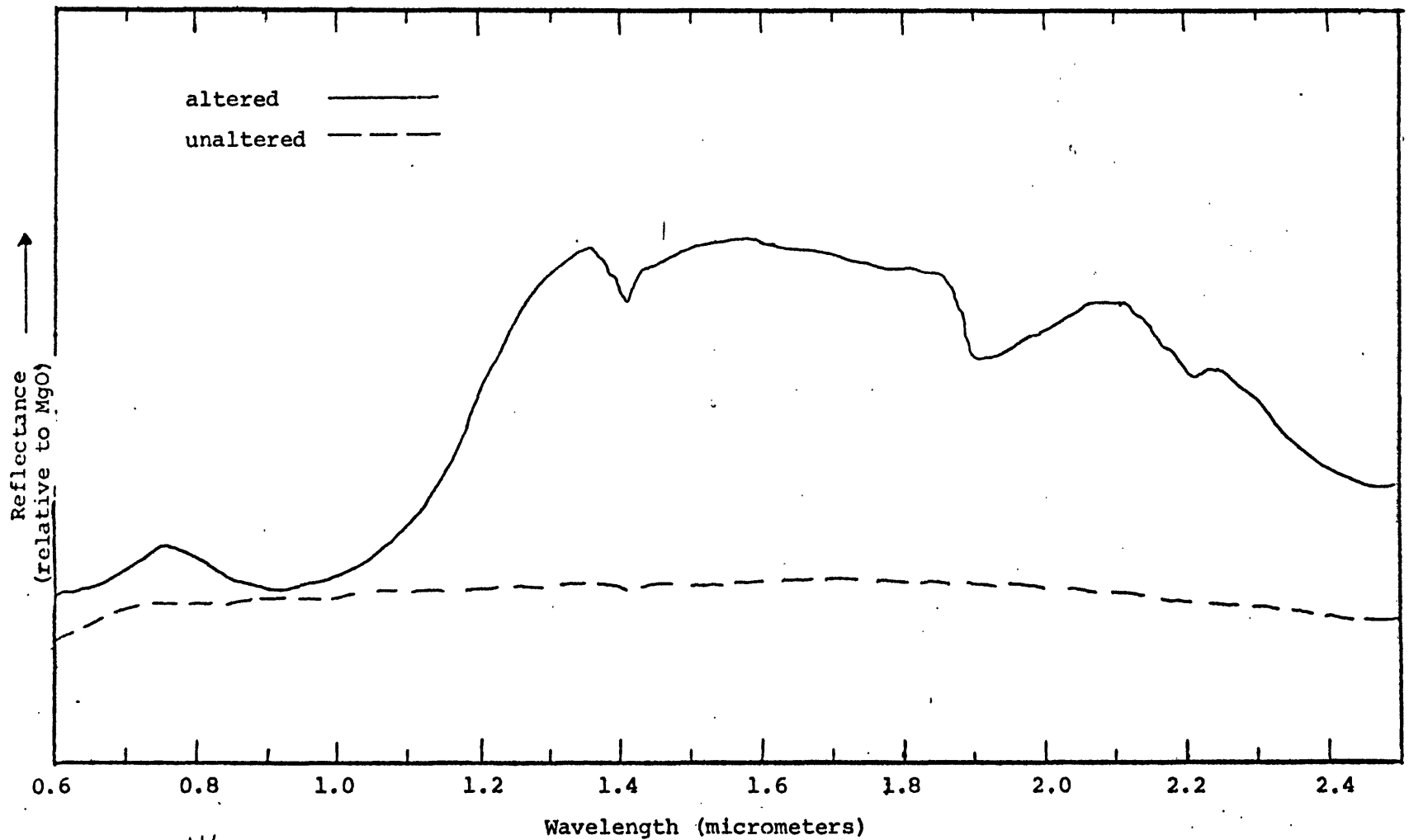
altered
unaltered
Reflectance
(relative to MgO)
0.6
0.8
1.0
1.2
1.4
1.6
1.8
2.0
2.2
2.4
Wavelength (micrometers)

Figure 14

illustrate the large spectral changes that result from weathering of the altered and unaltered cherts. The broad absorption band between 0.85 μm and 1.05 μm in the altered chert spectrum results from the ferric iron of the limonite coatings, and is enhanced by the high albedo of the bleached rock. However, spectral features are usually much more prominent in the laboratory spectra than in the in situ spectra, and caution must be used in judging spectral characteristics due to the small sample size (laboratory spectra were recorded on a Cary 14 spectrophotometer; for details on the operation, see Hunt and Salisbury, 1970).

The Copper Basin and Copper Canyon alteration halos, as depicted in the CRC (fig. 8) make a useful comparison. The alteration halo at Copper Basin is larger, and the green pixels are generally darker than at Copper Canyon. This difference is consistent with the relative amounts of limonite coatings observed in the two areas. Two geologic factors may explain the relative prominence of limonite at Copper Basin. First, this is a supergene porphyry copper deposit, and would have more surficial effects than Copper Canyon, which is predominantly of hypogene origin. Secondly, the variegated Harmony formation has more minerals that are susceptible of weathering to iron-oxides than the relatively homogeneous chert of the Scott Canyon and Pumpernickel formations at Copper Canyon.

The chief obstacle to remote alteration mapping in the Battle Mountain range is rocks of the Havallah formation. Green areas in the CRC, corresponding to the Havallah formation, are

located in the southwestern portion of the Battle Mountain range and throughout the northwestern corner of the image (fig. 8). Laboratory reflectance spectra were taken for three different lithologies within the Havallah formation: a quartzitic limestone, a dark blue-black chert, and a thin-bedded sandstone. The spectra for all three lithologies (fig. 15) indicate absorption by ferric iron, as shown by the steep fall-off below 0.8 μm, although only the chert spectrum exhibits a strong absorption band at 0.87 μm. However, intense absorption bands are not present in the 2.2 μm region, as was noted in the spectra of the altered Harmony and Scott Canyon formations (figs. 13 and 14), suggesting the usefulness of the 2.2 μm region in discriminating altered from unaltered limonitic rocks in the Battle Mountain area.

Shoshone Range

Several noteworthy, though small, mineral deposits are depicted in the CRC image within the Shoshone Range. The breccia pipes at Horse Canyon and Pipe Canyon (fig. 6, site J) are visible as a few green pixels on the southeast-facing slope in the eastern part of the range. These breccia pipes are composed of coarse to fine breccia of Tertiary sedimentary and igneous rocks that have been recrystallized, silicified, and have casts of pyrite and dark coatings of limonite on the exposed rock surfaces. On the southeastern sun-facing slope of Maysville Canyon, the Pittsburgh mine and the Blue Dick mine are depicted, as well as the Dean mine further to the north. To the

15

Figure - Laboratory reflectance spectra of specimens of three different limonitic lithologies of the Havallah formation. A, quartzitic limestone with a dark brown limonitic weathering rind more than 1 mm thick from Timber Canyon (fig. 4); B, dark blue-black chert, criss-crossed with quartz veins with a multi-colored surficial coating of limonite from a ridge 1.5 km west of Rocky Canyon (fig. 4); C, thin-bedded sandstone with a tan limonitic coating from the east side of the Buffalo Range (fig. 2).

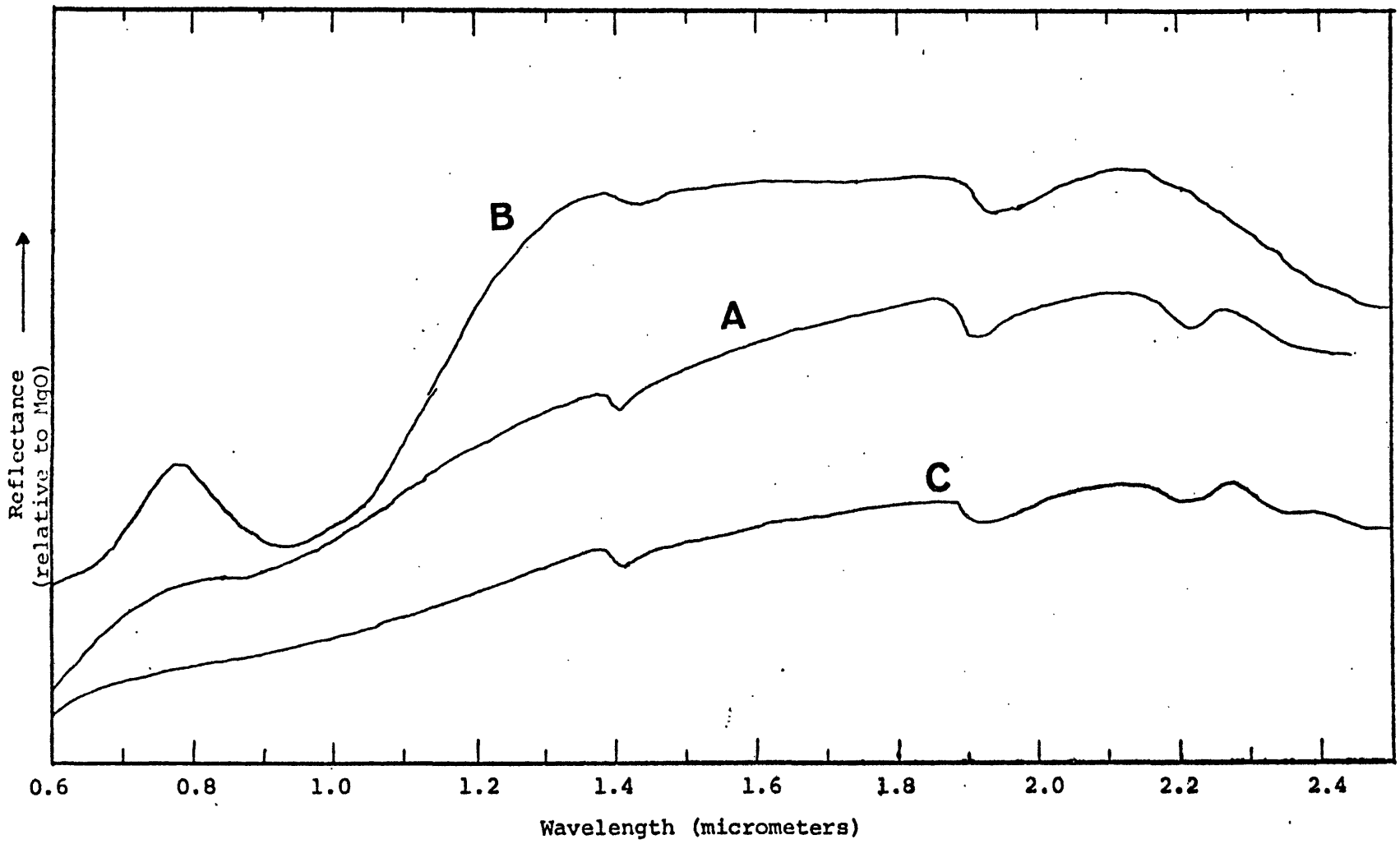
B
A
C
Reflectance
(relative to MgO)
0.6
0.8
1.0
1.2
1.4
1.6
1.8
2.0
2.2
2.4
Wavelength (micrometers)

Figure 15

west, the Hilltop district and the Bullion district (fig. 6, sites C and D), which are associated with an altered intrusive body, are mapped in the dark green separation (fig. 7). A large portion of the green area depicted in the CRC image for these two districts is occupied by the altered intrusive rocks.

The principal problem in the central Shoshones is that unaltered limonitic Valmy quartzite is similiar spectrally to the altered Valmy chert and quartzite. Thus, most of the green pixels visible in the CRC image (fig. 6) within the central spine of the Shoshone Range, represent unaltered rocks, except for the above mentioned mine sites. In situ spectral reflectance measurements demonstrate the source of this problem. A field spectrum for altered Valmy quartzite breccia from the Hilltop mine is almost identical to a field spectrum for unaltered limonite-coated Valmy quartzite (fig. 16). Both rock types have iron-absorption bands below 0.8 μm and near 0.9 μm, high reflectance near 1.6 μm, and no sizeable 2.2 μm band. These admittedly sparse field measurements are consistent with the large number of green pixels in the unaltered areas.

Spectra representing the unaltered limonitic Cataeno tuff and the Tertiary basaltic andesite(fig. 6, sites Tc and I), have a different spectral character than the altered rocks. An in situ spectrum for the Cataeno tuff (fig. 17) reveals the steep fall-off below 0.8 μm as a result of the surficial coating of iron, but the ferric iron absorption band at 0.87 μm is weak, and the reflectance maximum at 1.6 μm is subdued relative to spectra of altered rocks.

16

Figure 4 - Comparison of *in situ* reflectance spectra of specimens of altered and unaltered Valmy quartzite. The altered specimen is a quartzite breccia from the Hilltop mine (site C, fig. 9). Note the slight 2.2 μm absorption band in the altered quartzite spectrum.

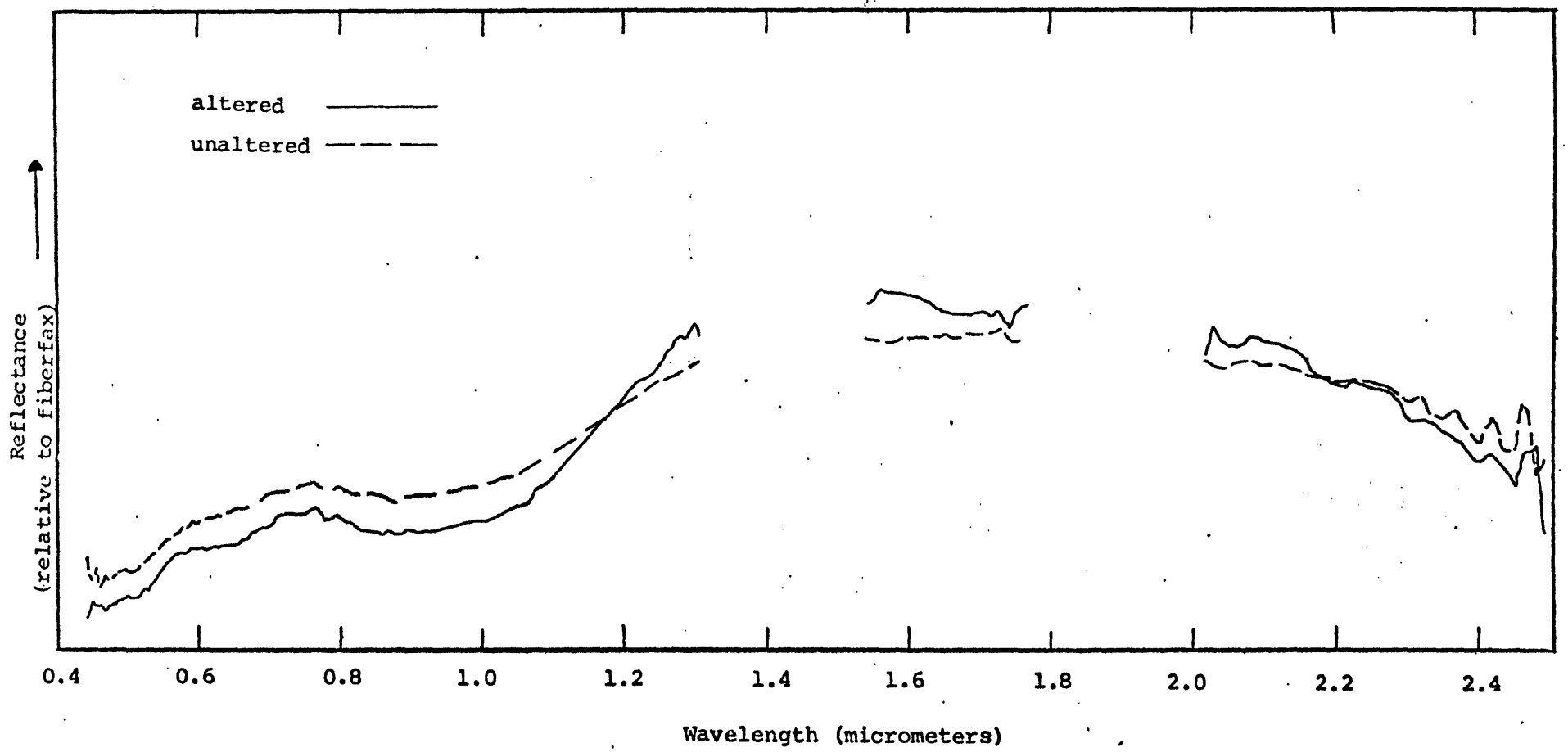
altered
unaltered
Reflectance
(relative to fiberfax)
0.4
0.6
0.8
1.0
1.2
1.4
1.6
1.8
2.0
2.2
2.4
Wavelength (micrometers)

Figure 16

17

Figure - In situ reflectance spectrum of a specimen of welded Cataeno tuff from south of Gold Acres.

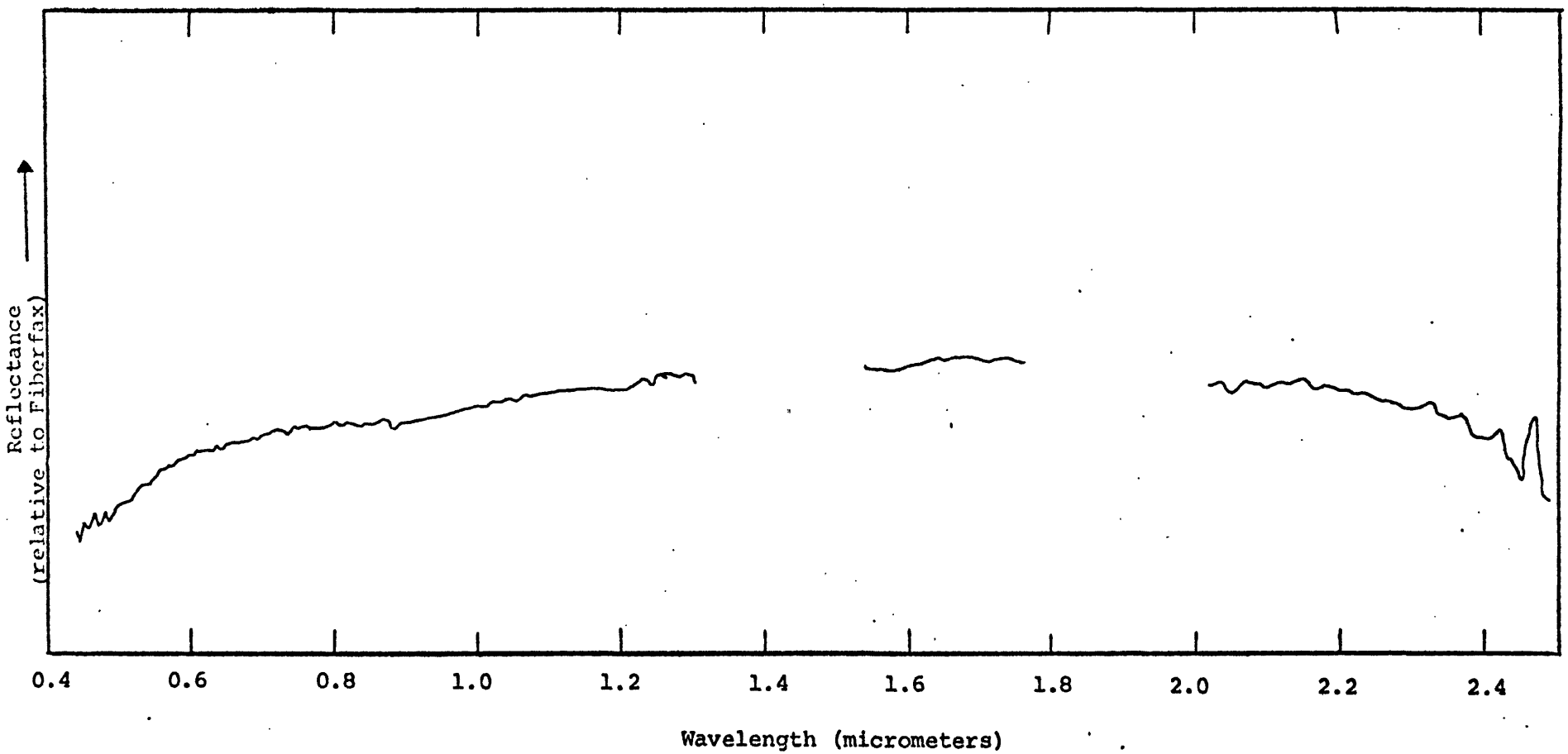
Reflectance
(relative to Fiberfax)
0.4
0.6
0.8
1.0
1.2
1.4
1.6
1.8
2.0
2.2
2.4
Wavelength (micrometers)

Figure 17

A laboratory spectra of the unaltered hematitic Tertiary basaltic andesite (fig. 18) shows similar spectral features. It is particularly important that neither of these unaltered rock spectra have a 2.2 μm absorption band, typical of most hydrothermally altered rocks.

An area of former hot spring activity within the Tertiary basaltic andesite near Fire Creek (fig. 6, site I) illustrates the large spectral changes resulting from hydrothermal alteration (fig. 18), even though the CRC depicts both the altered and unaltered basaltic andesite as green (fig. 6). First, the overall albedo of the altered rock is increased, which contributes to the intensity of the absorption bands. The ferric-iron band near 0.87 μm, a hydroxyl band at 2.2 μm, and several intense water absorption bands at 1.5 μm and 1.9 μm, are well defined in the laboratory spectrum for the altered rock (fig. 18). Whereas the water absorption bands are unavailable to remote sensing devices, a scanner with a longer wavelength capability than the MSS should be useful for discriminating these unaltered and altered volcanic rocks.

Perhaps the most significant omission of a known altered area from the CRC image within the four test sites in the Great Basin is the Gold Acres-Tenabo mining districts at the eastern margin of the Shoshones (fig. 6, sites E and F). The deposits are well above the spatial resolution capabilities of the MSS, and they appear bleached on the Landsat color-infrared composite (fig. 3), yet, only a band of a few scattered dark green pixels surrounded by some lighter greens are present here in the Linoscan color separation. Furthermore,

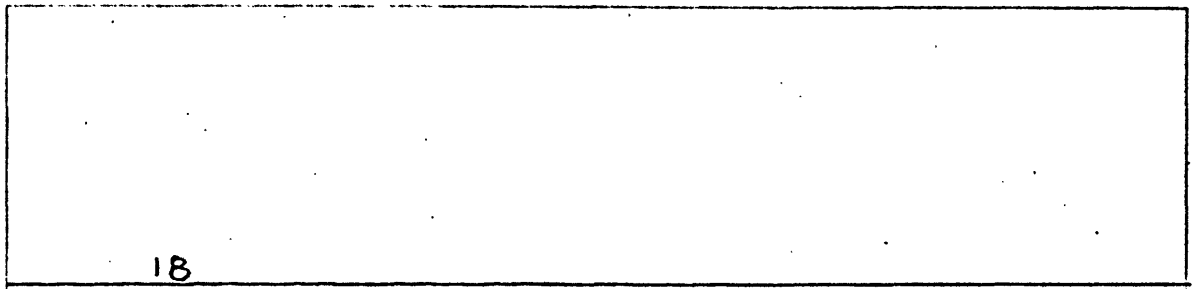

18

Figure . - Laboratory reflectance spectra of specimens of altered and unaltered Tertiary basaltic andesite from southwest of Beowawe, Nevada. The altered specimen is from an altered area by Fire Creek (site I, fig. 6).

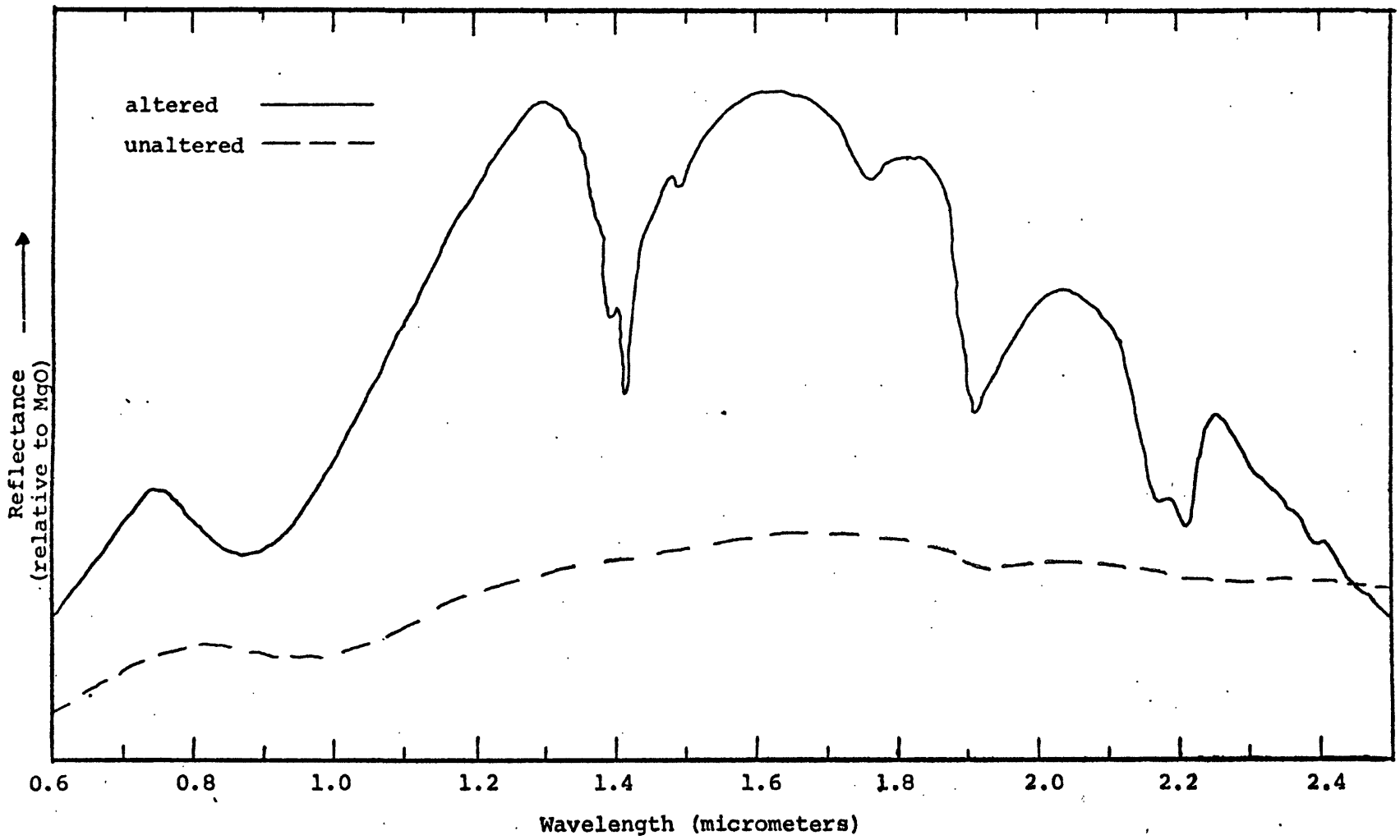
altered
unaltered
Reflectance
(relative to MgO)
0.6
0.8
1.0
1.2
1.4
1.6
1.8
2.0
2.2
2.4
Wavelength (micrometers)

Figure 18

some of the few green areas depicted at Gold Acres represent apparently unaltered rocks, especially in the western part, which consists predominantly of unaltered limonitic Valmy quartzite. At Tenabo, very little of the alteration is mapped, even in the yellow-green separation (fig. 7.).

Apparently, i.e. The main reason hydrothermal alteration is not detected by the CRC image in the Gold Acres area is the general paucity of limonite. The eastern side of the deposit is underlain by Wenban limestone that has been altered to tactite. The rock is uniformly light gray, and in situ spectra show no evidence of limonite absorption features. To the west, chert, quartzite, and greenstone of the Valmy formation and the Elder sandstone are the main host rocks. Limited in situ spectra of these rocks display no prominent iron-absorption, nor a prominent 2.2 μm absorption band, though kaolinization is reported to occur in these rocks.

Considering that unaltered Valmy quartzite west of the Gold Acres deposit is sufficiently limonitic to be detected in the CRC, the general absence of limonite in the Gold Acres area is notable. The other disseminated gold deposit in the CRC image at Cortez is largely obscured by the workings. Perhaps, i.e. The supergene processes that apparently redistributed the metals at Gold Acres (Wrucke and Armbrustmacher, 1975, p. 6) may also be responsible for leaching iron from the surface. If these processes are common to other disseminated gold deposits, the MSS will not be useful for discriminating this type of alteration.

SUMMARY

The objective of this NASA follow-on experiment was to test using color-ratio composites of Landsat images for mapping hydrothermal alteration under a variety of geologic and environmental conditions. In that regard, the following conclusions have been reached for the northwestern part of the Battle Mountain-Eureka mineral belt:

1. Limonitic alteration halos associated with two copper porphyry deposits were successfully mapped at Battle Mountain. Alteration halos from both a hypogene system at Copper Canyon and a supergene system at Copper Basin are recognizable in the composite. As would be expected, the areal extent of the limonitic coatings was more evident at the supergene deposit. Both copper porphyry deposits are located in sedimentary rock units that commonly have ferruginous coatings, yet, in most cases, the hydrothermally-derived limonite was distinguishable in the CRC from sedimentary limonite.

2. Large format playback images with pixel sizes from 200-400 µm provided details of spatial resolution and color separation unachievable on enlargements from 70 mm film chips. Details of the alteration halos, such as topographic shadowing and many small altered areas of 1-2 pixels in size, could only be resolved in the large format images.

3. Two aspects of the alteration halos of the porphyry copper deposits were not mapped on the CRC. Topographic shadowing occurred in the CRC on northwest-facing slopes greater than 20 degrees, in spite of the ratio processing. The steep topography and mid-September date of the image and its consequent low sun angle all appear to have contributed to this problem. A second cause for the white areas in the CRC image is the absence of a limonite altered rock north and west of the pit at Copper Basin that has not been previously mapped as a separate alteration unit. Atmospheric corrections applied to the CRC images may be a possible way to minimize topographic effects on the ratio images.

4. The vegetation cover, consisting predominantly of low ground cover, is fairly dense and uniform over the entire area. The effect of this vegetation in the CRC image is apparently to decrease the enhancement that can be achieved by contrast stretching of the MSS 5/6 ratio values. Because of its higher spectral radiance contrast, MSS 4/6 is not degraded by the severe stretches needed to enhance the pixels representing limonitic materials. Thus, in our opinion, the optimum CRC image for the study area consists of MSS 4/5 as blue, MSS 4/6 as yellow, and MSS 6/7 as magenta using diazo films. The side effect of using MSS 4/6 is to include more limonitic rocks that are not altered.

5. The dissimenated gold deposits at Gold Acres is not depicted in the CRC image. The area has an overall absence of limonite in comparison with other unaltered rocks, suggesting the dissemination process also may have removed the iron.

6. Unaltered limonitic rocks pose the biggest obstacle to regional alteration mapping in this area. Some of these rocks, such as the Cataeno tuff and those of the Havallah formation, appear to be separable using bandpasses near 1.6 μm and 2.2 μm. Other limonitic rocks, such as the Valmy quartzite, have spectra almost identical to the altered rocks, and are probably not separable even in these wavelength regions.

References Cited

Blodgett,H.W.,Brown, G. F.,and Moik, J.G., 1975, Geological mapping in northwestern Saudi Arabia using Landsat multispectral techniques: NASA Tech, Doc. No. X-923-75-206 21 p.

Cronquist, Arthur, Holmgren, Arthur H., Holmgren, Noel H., and Reveal, J.L., 1972, Intermountain flora - Vascular plants of the intermountain west, U.S.A., vol. 1: Harper Publishing Company, Inc., 270 p.

Gilluly, James, and Gates, Olcott, 1965, Tectonic and igneous geology of the northern Shoshone Range, Nevada, with sections on Gravity in Crescent Valley by Donald Plouff, and Economic Geology by K.B. Ketner: U.S.Geol. Survey Prof. Paper 465, 153 p.

Goddard, E.N., and others, 1948, Rock-color chart: Washington, D.C., Natl. Research Council, 6p. (republished by Geol. Soc. America, 1951; reprinted, 1970, 8p.)

Goetz, A.F.H., Billingsley, F.C., Gillespie, A.R., Abrams, M.J., Squires, R. L., Shoemaker, E. M., Lucchitta, I., and Elston, D. P., 1975, Application of ERTS images and image processing to regional geologic problems and geologic mapping in northern Arizona:

Jet Propulsion Lab. Tech. Rept. 32-1597, Pasadena, CA. 188p.

Hack, J.T., and Goodlet, J.C., 1960, Geomorphology and forest ecology of a mountain region in the Central Appalachians: U.S. Geol. Survey Prof. Paper 347, 66 p.

Horton, R.C., 1966, Statistical studies of the distribution of mining districts in Nevada, in AIME Pacific Southwest Mineral Conference, Sparks, Nev.: Nevada Bur. Mines Rept. 13, Pt. A., p. 109-123.

Hunt, G.R., and Salisbury, J.W., 1970, Visible and near-infrared spectra of minerals and rocks: I - Silicate Minerals: Mod. Geol., vol. 1, p. 283-300.

Hunt, G.R., Salisbury, J.W., and Lenhoff, C.J., 1971, Visible and near-infrared spectra of minerals and rocks: III - Oxides and Hydroxides: Mod. Geol., vol. 2, p. 195-205.

Hunt, G.R., Salisbury, J.W., and Lenhoff, C.J., 1973, Visible and near-infrared spectra of minerals and rocks: VI - Additional Silicates: Mod. Geol., vol. 4, p. 85-106.

Hunt, G.R., 1977, Spectral signatures of particulate minerals in the visible and near-infrared: Geophys., vol. 42, no. 1, p. 501-513.

Jaegar, E.C., 1969, Desert wild flowers: Stanford Univ. Press, Stanford, CA., 322 p.

Jones, E.C., Wrucke, C.T., Holdsworth, Brian, and Suczek, C.A.,1978, Revised ages of chert in the Roberts Mountain allochthon, northern Nevada [abs.]: Geol. Soc. Amer. Abstracts with programs (in press).

Knipling, E.G., 1970, Physical and physiological basis for the reflectance of visible and near-infrared radiation from vegetation: Remote Sensing of Environ., vol. 1, no. 3, p. 155-159.

McKee, E.H., and Silberman, M.L., 1970, Geochronology of Tertiary igneous rocks in central Nevada: Geol. Soc. Amer. Bull., vol. 81, no. 8, p. 2317-2328.

Munsell Color Company, 1969, Munsell book of color, neighboring hue edition, matte finish collection: Baltimore, MD (looseleaf, unnumbered pages).

Offield, T.W., 1976, Remote sensing in uranium exploration: Amer. Inst. Min. Engr. (AIME) proc. of mtg., 30 Mar-2 Apr 1976, Vienna, Austria, p. 731-744.

Preston, Richard J., 1968, Rocky Mountain Trees: Dover Publications, Inc., New York, 285 p.

Raines, G. L., 1976, A porphyry copper exploration model for northern Sonora, Mexico [abst.]: Geol. Soc. Amer. Abstracts with programs, vol. 8, no. 6, p. 1057.

Roberts, R.J., 1964, Stratigraphy and structure of the Antler Peak quadrangle, Humboldt and Lander Counties, Nevada: U. S. Geol. Survey Prof. Paper 459-A, 90 p.

Roberts, R.J., and Arnold, D.C., 1965, Ore deposits of the Antler Peak quadrangle, Humboldt and Lander Counties, Nevada: U. S. Geol. Survey Prof. Paper 459-B, 93 p.

Roberts, R.J., 1966, Metallogenic provinces and mineral belts in Nevada: Nevada Bur. Mines Rept. 13, Pt. A, p. 47-72.

Roberts, R.J., Radtke, A.S., and Coats, R.R., 1971, Gold-bearing deposits in north-central Nevada and southwestern Idaho with a section on Periods of Plutonism in north-central Nevada, by M.L. Silberman and E.H. McKee: Econ. Geol., vol. 66, no. 1, p. 14-33.

Rowan, L.C., Wetlaufer, P.H., Goetz, A.F.H., Billingsley, F.C., and Stewart, J.H., 1974, Discrimination of rock types in Nevada by the use of ERTS images: U. S. Geol. Survey Prof. Paper 883, 35 p.

Rowan, L.C., Goetz, A.F.H., and Ashley, R.P., 1977, Discrimination of hydrothermally altered and unaltered rocks in visible and near-infrared multispectral images: Geophysics, vol. 42, no. 3, p. 522-535.

Sayers, R.W., Tippett, M.C., and Fields, E.D., 1968, Duval's new copper mines show complex geologic history: Mining, Engr., p. 55-62.

Shawe, D.R. and Stewart, J.H., 1976, Ore deposits related to tectonics and magmatism, Nevada and Utah: Am. Inst. Mining, Metal., and Petroleum Engineers Trans., vol. 260, no. 3, p. 225-231.

Siegal, B.S., and Goetz, A.F.H., 1977, Effect of vegetation on rock and soil type discrimination: Photogram. Engr. and Remote Sensing, vol. 43, no. 2, p. 191-196.

Silberman, M.M., Stewart, J.H., and McKee, E.H., 1976, Igneous activity, tectonics, and hydrothermal precious-metal mineralization in the Great Basin during Cenozoic time: Am. Inst. Mining, Metal., and Petroleum Engineers, Soc. Mining Engineers Trans., vol. 260, no. 3, p. 253-263.

Stewart, J.H., and Carlson, J.E., 1976, Geologic map of north- central Nevada: Nevada Bur. Mines and Geol. Map 50.

Stewart, J.H., and Suczek, C.A., 1977, Cambrian and Late Pre-Cambrian paleogeography and tectonics in the western United States, in Stewart, J.H., Stevens, C.H., and Fritsche, A.E., eds., Paleozoic

paleogeography of the western United States: Soc. Econ. Paleontologists and Mineralogists, Pacific Coast Paleogeography Symposium I, p. 1-17.

Theodore, T.G., and Roberts, R.J., 1971, Geochemistry and geology of deep drill holes at Iron Canyon, Lander County, Nevada, with a section on Geophysical logs of drill hole DDH-2, by Charles J. Zablocki: U. S. Geol. Survey Bull. 1318, 32 p.

Theodore, T.G., Silberman, M.L., and Blake, D.W., 1973, Geochemistry and K-Ar ages of plutonic rocks in the Battle Mountain mining district, Lander County, Nevada: U. S. Geol. Survey Prof. Paper 798-A, 24 p.

Theodore, T.G., and Blake, D.W., 1975, Geology and geochemistry of the Copper Canyon porphyry copper deposit and surrounding area, Lander County, Nevada: U. S. Geol. Survey Prof. Paper 798-B, 86 p.

Vincent, R.K., 1977, Uranium exploration with computer-processed Landsat data: Geophysics, vol. 42, no. 2, p. 536-541.

Wrucke, C.T., 1974, Geologic map of the Gold Acres-Tenabo area, Shoshone Range, Lander County, Nevada: U.S. Geol. Survey Misc. Field Studies Map, MF-647.

Wrucke, C.T., and Armbrustmacher, T.J., 1975, Geochemical and geologic relations of gold and other elements at

the Gold Acres open-pit mine, Lander County, Nevada: U.S. Geol. Survey Prof. Paper 860, 27 p.

Wrucke, C.T., and Silberman, M.L., 1975, Cauldron subsidence of Oligocene age at Mt. Lewis, northern Shoshone Range, Nevada: U. S. Geol. Survey Prof. Paper 876, 20 p.